The Relation between Land-Cover and the Urban Heat Island in Northeastern Puerto Rico

by

David J. R. Murphy

A thesis submitted in partial fulfillment
of the requirements for the
Master of Science Degree
State University of New York
College of Environmental Science and Forestry
Syracuse, New York
March 2007

Approved: Faculty of Environmental science

____
Myrna H. P. Hall, Major Professor

____
Charles A. S. Hall, Major Professor

____
Sarah Vonhof, Chair,
Examining Committee

____
Richard Smardon, Faculty Chair

____
Dudley J. Raynal, Dean,
Instruction and Graduate Studies

UMI Number: 1442457

ProQuest Information and Learning Company
300 North Zeeb Road
P.O. Box 1346
Ann Arbor, MI 48106-1346

Acknowledgements

I would like to thank Myrna Hall for her tireless effort throughout my graduate career, especially for her attention during the last few months when I was finishing my thesis. Many thanks also to Charles Hall for developing and supporting this project.

I would also like to thank Gordon Heisler for his meteorological expertise, without which this project would not have been completed. Also, thanks to Steve Stehman for his statistical expertise and incite, which allowed me to address issues like equipment calibration and data analysis with confidence.

A debt of gratitude is owed to my officemates and colleagues within the ESF community. Positive, yet merciless peer-criticism (especially from my fellow graduate students and advisors) was by far the best way for me to develop projects, ascertain good analysis ideas, sieve through bad ideas, and, eventually, develop a great final product. I thank everyone involved in these formative experiences.

Many thanks also to my father Paul, my mother Dana, and my brother Ben for their continued support throughout my graduate career.

Table of Contents

List of Tables

Chapter 1:
Literature Review

Chapter 2:
The Relation between Land-Cover and the Urban Heat Island in Northeastern Puerto Rico

List of Figures

Chapter 1:
Literature Review

Chapter 2:
The Relation between Land-Cover and the Urban Heat Island in Northeastern Puerto Rico

Abstract

Murphy, David J.R. The Relation between Land-Cover and the Urban Heat Island in Northeastern Puerto Rico. Typed and bound thesis: 98 pages, 8 tables, 36 figures, 2007.

My objectives in this study are: (1) to quantify the timing of the peak urban heat island (UHI), (2) to explore correlations between air temperature and land-cover, (3) to assess the geographic range of the UHI, and (4) to predict geographic growth of the UHI in the future.

To do this, I collected in situ temperature data using mobile and fixed-station transects. I used this data along with land-cover data to correlate upwind vegetation with temperature measurements. By predicting urban growth over time I was able to track the geographic expansion of the UHI.

My results indicate: (1) San Juan exhibits a nocturnal UHI, (2) canopy cover is needed to reduce UHI effects during the daytime, (3) the UHI effect may impede cloud formation within the Luquillo Mountains, and (4) future urbanization will intensify the UHI effect at the Luquillo Mountains, exacerbating its impact on cloud formation.

Murphy, David J.R. Master of Science March 2007

Major Professor: Myrna H. P. Hall

Department of Environmental Studies, State University of New York, College of Environmental Science and Forestry, Syracuse, New York.

Signature of Major Professors: ___________________________

Myrna H. P. Hall

____

Charles A. S. Hall

Chapter 1: Literature Review

1. Introduction

In 2007, for the first time globally, urban populations are projected to outnumber rural populations (UN-POP 2004). The growth of urban populations results in the growth of urban areas, and in the United States, urbanized areas are projected to increase from 3.8% to 8.1% of total land area by 2050, which will impact not only air and water quality, but also human well-being (Nowak and Walton 2005). One such impact of regional urbanization is warmer air temperatures, a phenomenon known as Urban Heat Islands (Stull 2000; Carbone 2004). Globally, the growth of urban populations and urban land area may produce quantifiable changes in the Earth's atmosphere. These changes along with, for example Montana's disappearing glaciers and Mediterranean desertification, are construed by many as direct results of the quantifiable changes occurring in the Earth's climate (Hall and Farge 2003; Millán et al. 2005).

Urban Heat Islands (UHI), my focus here, are a product of anthropogenic land-cover modifications. Urban surfaces, such as concrete, asphalt, and brick, change the natural sun-earth energy budget causing urban areas to have warmer temperatures than surrounding suburban or rural areas in the same locale (Douglas 1983; Stull 2000; Carbone 2004). The UHI phenomenon is well documented around the world including the North American cities of Tucson, Phoenix, Montreal, Baltimore, Chicago, and Vancouver (Oke and East 1971; Landsberg and Brush 1980; Comrie 2000; Hawkings et al. 2004; Fast et al. 2005; Johnston 2005; Hedquist and Brazel 2006; Heisler et al. 2006).

Urban Heat Islands are undesirable for numerous reasons. Warmer temperatures in urban areas increase the metabolic stress of people already living at the edge of a safe and comfortable gradient space for humans. Human deaths associated with recent heat waves in Chicago (1999), India (2003), and France (2004, 2006) illustrate the severity of this issue.

Another undesirable attribute of UHIs is that as people mitigate the increase of even only 1°C or 2°C in urban areas there are escalating energy costs for cooling (Akbari et al. 2001). Estimates by Akbari et al. (2001) conclude that efforts in the U.S. to mitigate UHIs nationwide could save 20 billion dollars spent on increased air conditioner use. Thus, mitigation of the UHI effect is important, not only for health-related issues, but also for reducing energy and dollar expenditures.

The cooling effects of evapotranspiration are frequently utilized to mitigate the UHI (Bounoua et al. 2004). ‘Green roofs’ or general urban ‘greening’ efforts are being instituted in many urban areas to utilize the natural cooling properties of vegetation. Akbari et. al. (1988) modeled the effect of increasing albedo (surface reflectivity) and tree coverage on cooling energy costs. He calculated that increasing albedo from 30% to 70% and adding 3 trees to the west and south sides of residences results in direct cooling energy savings of 20% per residence.

Chicago has been actively pursuing ‘greening’ efforts over the past 15 years. Since 1991 Chicago has planted 400,000 new trees within the city limits. These trees accomplish many goals, including an estimated annual: (a) removal of airborne particulate matter from 31,000 vehicles, (b) production and release of 23 tons of oxygen into the local atmosphere, and (c) mitigation of UHIs, which cost the city an estimated 150 million dollars per degree increase (Johnston 2005; McPherson 1997).

Some of the most rapid population growth and urbanization is occurring in the developing nations of the tropics, but most of the UHIs studied to date are located in temperate, developed nations. UHIs will effect and be affected by trade winds, sea-breeze effects, and rainfall patterns dependent on the formation of orographic clouds. Moreover, increasing temperatures can change the demand for energy used in cooling from a seasonal expense to an annual expense. To understand the interactions between coastal-tropical climates, land-cover, and UHIs better, I have conducted an empirical study of the UHI created by the metropolitan area of San Juan, Puerto Rico.

a. Historical Development and Land-Cover Change in Puerto Rico

Puerto Rico is the smallest of the Greater Antilles Island chain located between the Caribbean Sea and the Atlantic Ocean, at 18° north latitude and 66° west longitude (Figure 1). San Juan, the capital and largest city, is located on the eastern half of the island along the north coast and receives trade-wind breezes from both the east and northeast.

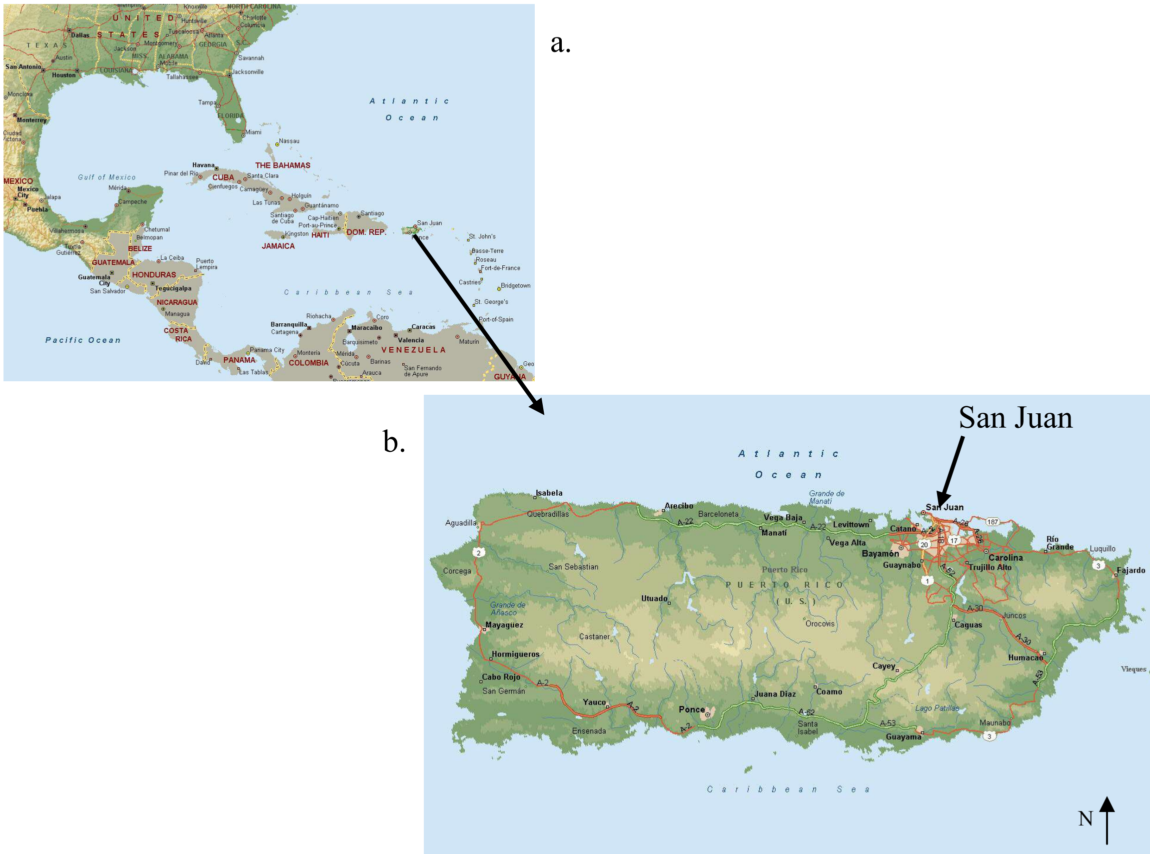

Figure 1. (a) The entire Antilles chain, starting in the northwest with Cuba, and ending just north of Venezuela; (b) the island of Puerto Rico (Microsoft Streets and Trips, 2005).

There are two mountain ranges on the Island: the 'Luquillo Mountains', which contain the Luquillo Experimental Forest (LEF), are located 17 kilometers east of the San Juan Metropolitan Area (SJMA) and have a maximum elevation of ~1100 meters (Figure 2). The Mid-Island Mountains begin about 60 kilometers southwest of San Juan, and extend throughout the center of the island, with a maximum elevation of ~1300 meters.

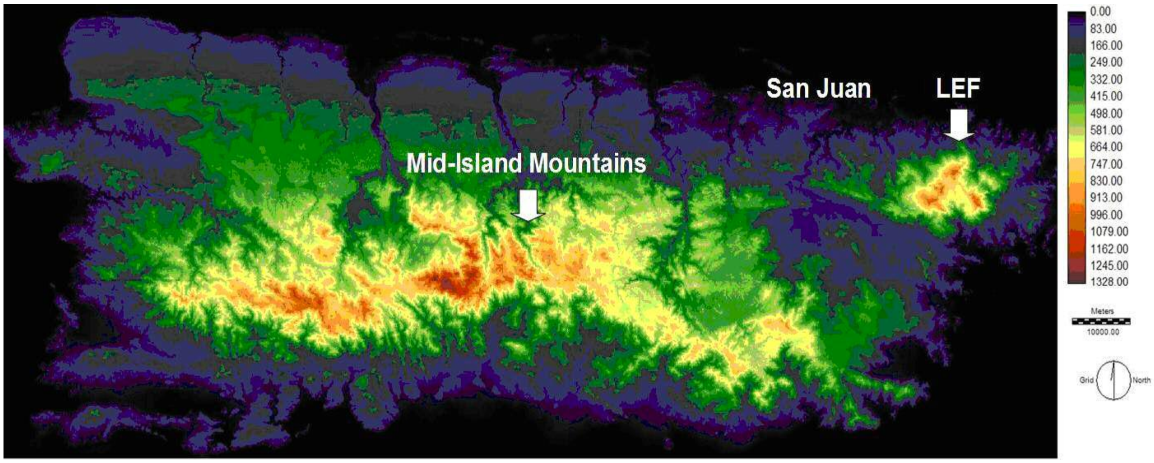

Figure 2. Digital Elevation map of Puerto Rico displaying mountains to the East and Southwest of San Juan, with the highest elevations in red (Helmer and Ruefenacht 2005).

Historically, most tropical regions followed the development patterns described by classical economist David Ricardo (1911), who observed that societies tend to use the best agricultural lands first, and then use increasingly more marginal lands as populations grow. For mountainous tropical islands, this means that the low, coastal, arable lands with the best protection from, and access to, the ocean were developed first. Old San Juan was the first major settlement in Puerto Rico, and it lies at the end of an isthmus that allows access to San Juan Bay. This area has good fortifications from either a sea or land attack, access to both the ocean and bay for food resources, and flat land for agriculture.

Prior to Spanish arrival in the 15th Century, the land cover of Puerto Rico was a mix of old growth forests and coastal marsh lands. The indigenous Tainos cleared only small patches of forest for their farming needs (Gomez and Ballesteros 1980). After the arrival of the Spanish, deforestation began for both timber and agricultural production, including: annual subsistence crops, sugar cane, pastures, coffee and bananas. By 1825, 65% of Puerto Rico was deforested, by 1899 - 80%, by 1931 - 91%, and by the late

1940's - 94% (Durland 1929; Gill 1931; Wadsworth 1950; Koenig 1953; Figure 3). Reforestation at higher elevations began in the mid-1900's as eroding soils forced farming and grazing to move back down the mountains (Aide et al. 1995).

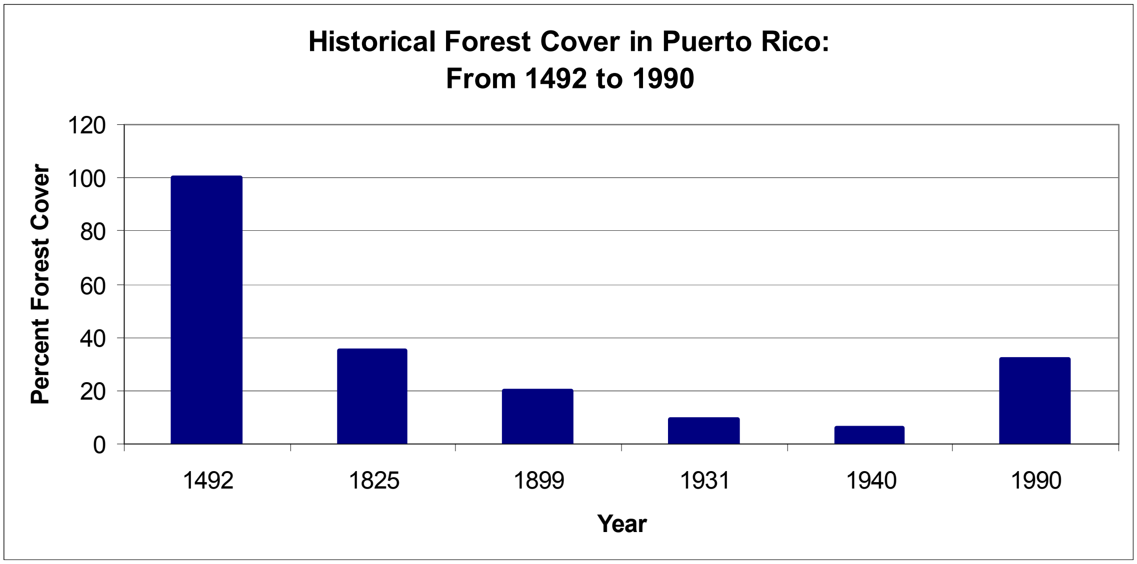

Figure 3. Percent forest cover in Puerto Rico from pre-Columbus to 1990.

Over the past fifty years, many other tropical nations have mimicked the Puerto Rican experience just described (Achard et al. 2002). However, over these same 50 years, Puerto Rico itself has been reforesting, due to the abandonment of an agriculture-based economy (Figure 4), and by 1990, 32% of the island had regained forest cover (Franco et al. 1997; van der Molen 2002). Urban areas, however, lost much of the vegetation that remained and the ratio of vegetative/non-vegetative cover within city limits decreased.

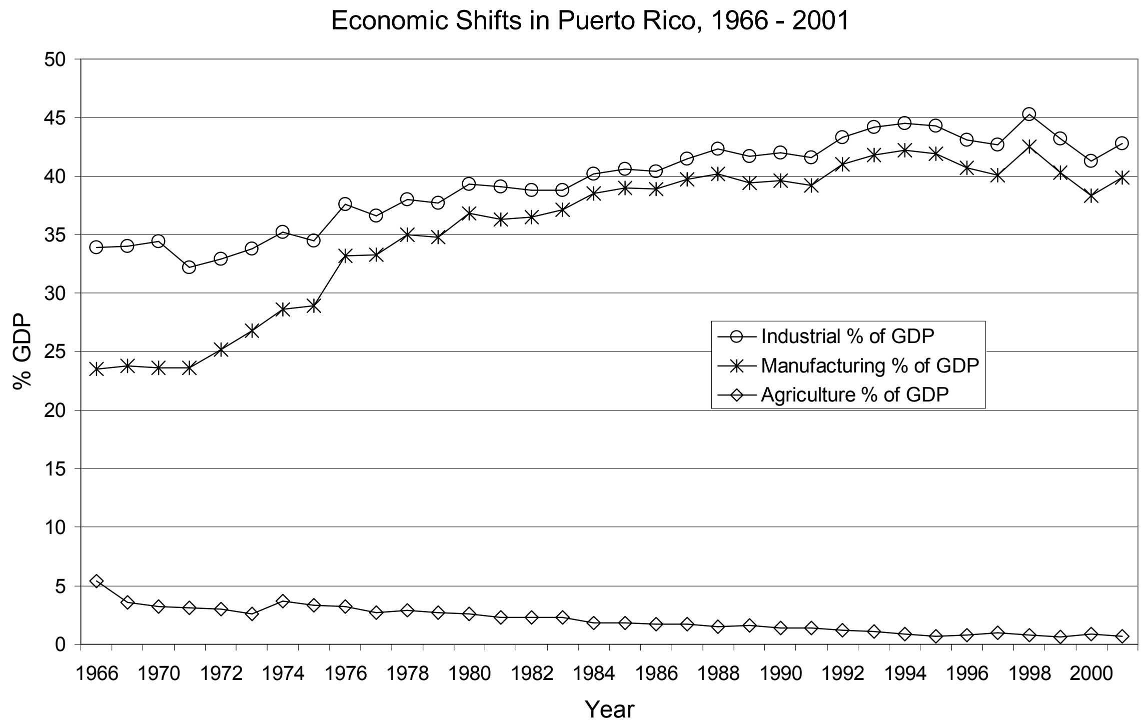

Figure 4. Comparison between three sectors of GDP in Puerto Rico since the mid-1960's (World Resources Institute).

The abandonment of an agriculture-based economy began with 'Operation Bootstrap', initiated in 1948 by Governor Munoz Marin to convert Puerto Rico from an agricultural economy to an industrial economy. Tax incentives and lenient environmental policies were used to draw companies and entire industries, such as pharmaceutical manufacturing, to Puerto Rico. 'Operation Bootstrap' succeeded in industrializing the Puerto Rican economy (Figure 4), and in doing so caused massive migrations to its urban areas. The 2000 census indicated that urban areas within Puerto Rico hold 94% of the total Puerto Rican population (UN-POP 2004; Figure 5). Industrialization and urban immigration resulted in the once cultivated agricultural land becoming fallow, allowing for the slow regeneration of forest cover.

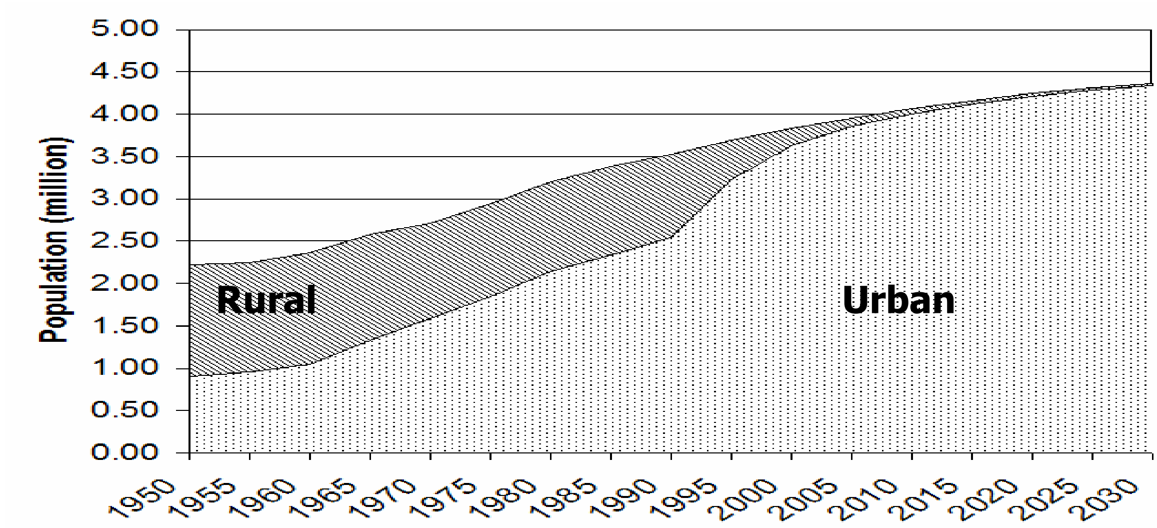

Figure 5. Past, present, and projected urban and rural populations within Puerto Rico (Puerto Rico, UN – POP 2003: UN-POP 2004).

2. Urban Heat Islands

Anthropogenic alterations to the earth surface causes microclimatic changes that result in the formation of Urban Heat Islands (Landsberg 1981). The most obvious of these changes is land-cover. Land-cover types common to urban areas, such as dark colored pavement, brick, and asphalt, absorb radiation during the day and release it during the evening, causing maximum temperature differences between urban and rural environments to occur at night (Chandler 1965; Oke and East 1971; Landsberg 1981).

UHIs are caused by changes in the sun-earth radiation balance. The radiation balance is formed by shortwave (visible light and ultraviolet) and longwave (infrared, i.e. thermal) radiation entering the Earth's atmosphere from space. This radiation can be reflected (e.g. off the tops of clouds), refracted (e.g. passing through atmospheric moisture), and/or absorbed by the Earth's surface (Lutgens and Tarbuck 2004; Figure 6). Cloud cover and the albedo (reflectivity) of land-cover are major determinants of how much of the incident radiation is reflected, refracted, or absorbed at any point on earth (Oke 1973; Stull 2000; Carbone 2004; Heisler et al. 2006).

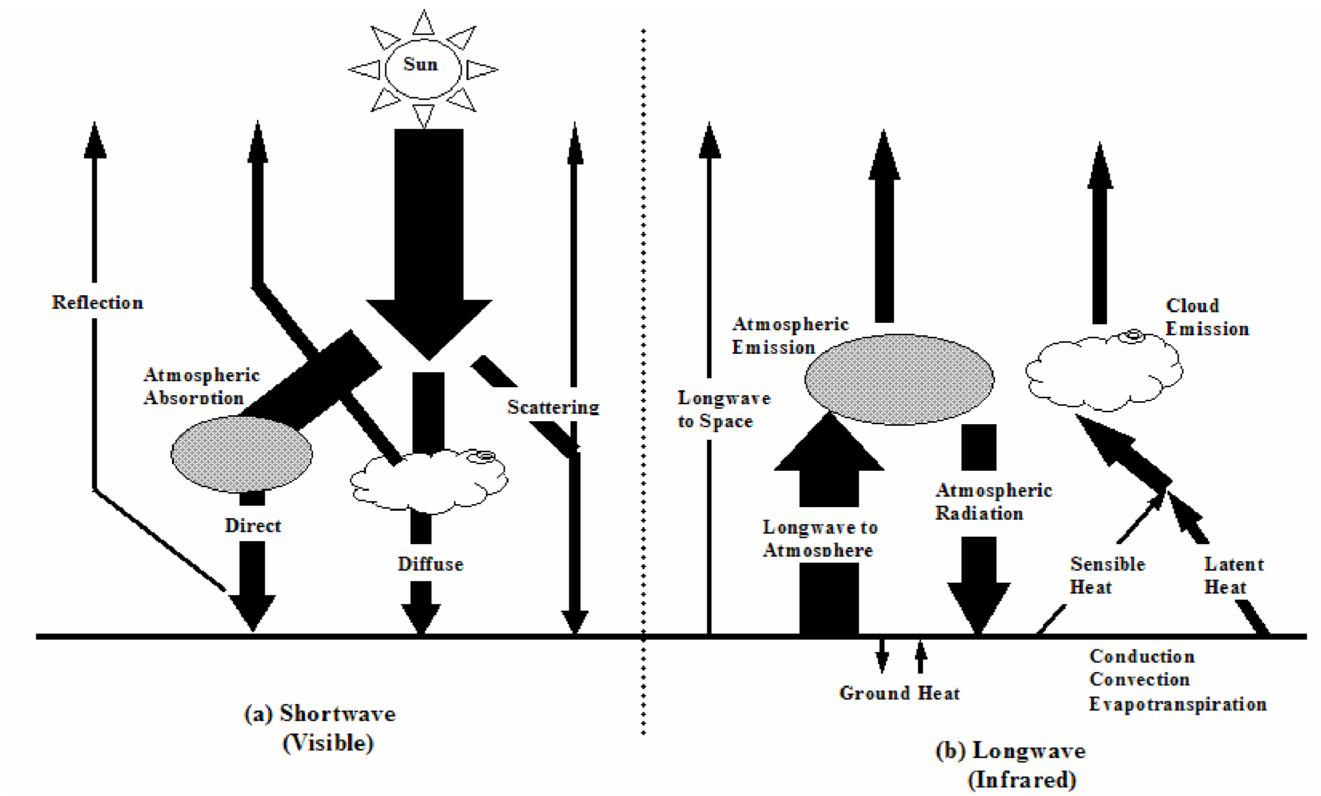

Figure 6. Conceptual diagram of the sun-earth radiation budget (from Lutgens and Tarbuck, 2004). During daylight hours, both shortwave and longwave radiation are present (a), but during the nighttime only the longwave radiation is present (b).

Fluxes of shortwave and longwave radiation between the atmosphere and the Earth's surfaces created by variable amounts of reflection, refraction, and absorption, cause imbalances in the radiation balance. Concrete, brick, asphalt, and other surfaces common to urban areas absorb longwave radiation during the day and reemit it at different rates during the evening, thus forming the UHI (Stull, 2000). The radiation balance is quantified by a net radiation value (Stull 2000; Carbone 2004), given as:

$$\text{Net Radiation} = (SW\uparrow - SW\downarrow) + (LW\uparrow - LW\downarrow)$$

where:

$SW\downarrow$ - Incident shortwave radiation reaching earth surface
$SW\uparrow$ - Reflected shortwave radiation (surface albedo * $SW\downarrow$)
$LW\downarrow$ - Longwave radiation emitted by sun and atmosphere
$LW\uparrow$ - Longwave radiation emitted by the earth surface

a. *Periodic Fluctuations of the Urban Heat Island*

1) DIEL UHI FLUCTUATIONS

Urban areas tend to remain warmer throughout the evening, making the diel range of air temperatures, i.e. the range in temperatures over a 24 hour period, smaller in urban areas when compared to surrounding rural areas in the same locale. Chandler (1965) studied the London UHI over a 10-year period. His study showed that on most days the difference in daily minimum temperature between an urban location and a rural location ($\Delta T_{minU\text{-}R}$) was larger than the difference in daily maximum temperature ($\Delta T_{maxU\text{-}R}$; Chandler 1965; Figure 7). This was caused by a lack of cooling in urban areas during the evening.

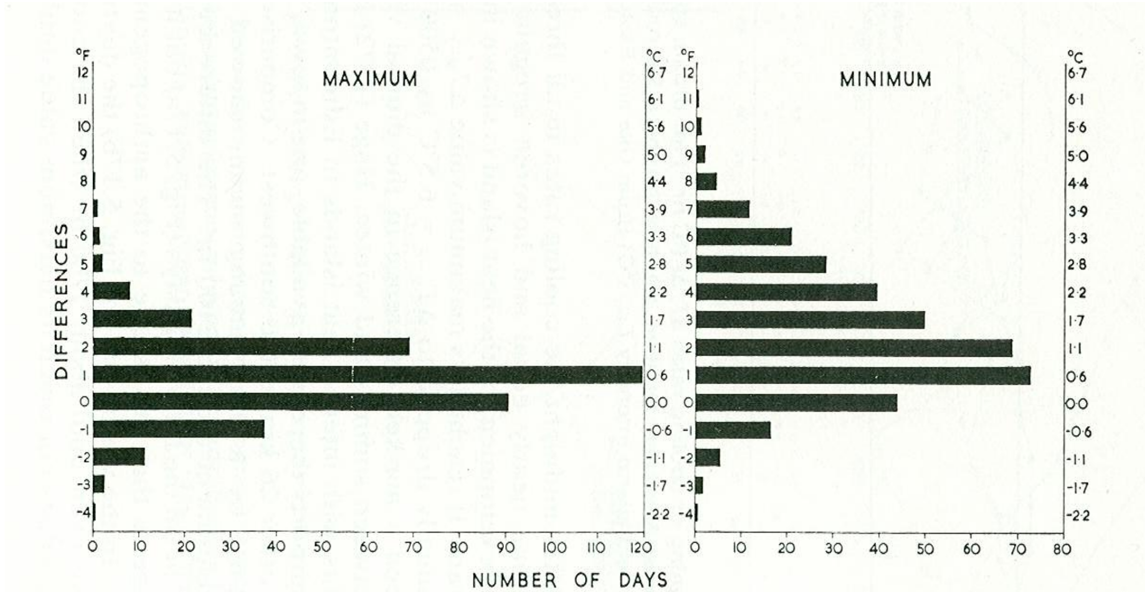

Figure 7. Difference in temperature between urban and rural areas ($\Delta T_{minU\text{-}R}$; $\Delta T_{maxU\text{-}R}$), represented as number of days per year, from a 10-year record in London, England (Chandler 1965).

Oke and East (1971) compared the winter diel cooling rates (°C/hour) for three meteorological stations placed in rural, suburban, and urban sites. Both the rural and suburban sites had cooling rates of at least -0.2 °C hour^{-1} between hours 1600 and 1700 (Figure 8). Temperature at the urban site actually increased until 2200 hours and did not cool until after 2200 hours. Reemission of longwave radiation by urban surfaces caused a 4.5 hour lag in the urban cooling rate.

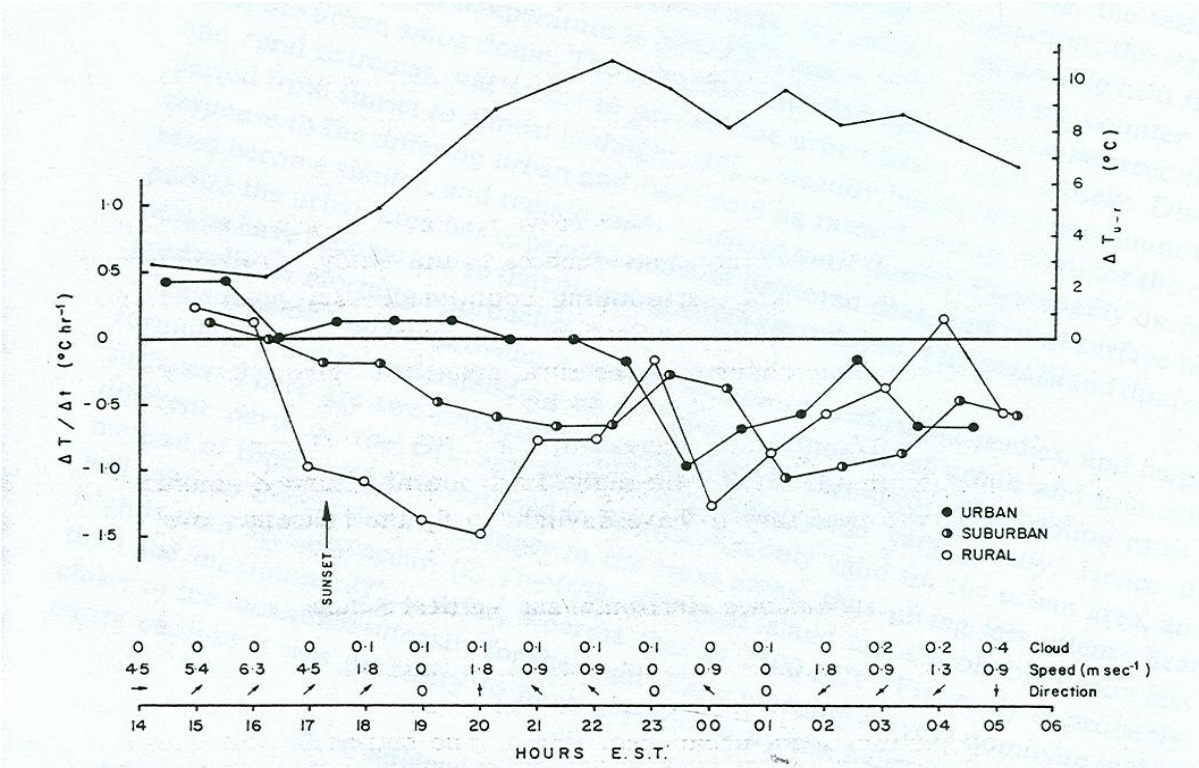

Figure 8. Urban, suburban, and rural cooling rates (°C hour^{-1}) and UHI intensity (ΔT_{U-R}) for a February night in Montreal, Canada (Oke and East 1971).

2) DAY TO DAY UHI FLUCTUATIONS

Anthropogenic heat release can cause day to day fluctuations in UHI intensity. Mitchell (1961) showed that differences in minimum diel temperature between the city of New Haven, Connecticut, and the neighboring airport (ΔT_{minU-R}) was consistent for all days except Sunday, for which it was half as great (Table 1a). Similar findings were reported by Landsberg and Brush (1980) who found a four-fold decrease in average temperature differences (ΔT_{aveU-R}) on Sundays between Baltimore City and the Baltimore-Washington International Airport during the winter (table 1b). Decreasing UHI intensity on Sunday is attributable to the lack of anthropogenic activity. Automobile commutes and office air conditioners, for example, release large amounts of heat into the atmosphere and are used less on Sunday's.

Table 1. (a) Max and min daily temperature differences between the city of New Haven, Connecticut, and the neighboring airport, stratified by days of the week, winters 1939 – 1943 (Mitchell 1961).

a.

	ΔT_{u-r} (°C)		
Day	max	min	Daily mean
Monday	0	1.1	0.6
Tuesday	0.1	1.3	0.7
Wednesday	0	1.2	0.6
Thursday	0	1.3	0.7
Friday	0	1.3	0.6
Saturday	0	1.2	0.6
Sunday	0.1	0.6	0.3

(b) Daily temperature differences stratified by days of the week between Baltimore City and Baltimore-Washington International Airport, 1971 – 1975 (Landsberg and Brush 1980).

b.

Day	Winter	Summer
Sunday	0.2	2.2
Monday	0.9	2.0
Tuesday	1.0	1.3
Wednesday	0.8	1.6
Thursday	0.7	1.4
Friday	0.7	1.4
Saturday	0.4	1.7
Mean	0.7	1.6
σ	1.7	1.7

3) SEASONAL UHI FLUCTUATIONS

Seasonal effects of the UHI can be observed, and are sometimes quantified as heating and cooling degree days. Heating and cooling degree days are a way to compare the need to heat in the winter or cool in the summer by quantifying the average departure from a threshold value of 18°C. Heating degree days (HDDs) are computed as the sum of daily average temperatures below 18°C (Quale and Diaz 1979). Cooling degree days

(CDDs) are computed as the sum of daily average temperatures above 18°C. Due to the warming effects of the UHI, there are usually fewer HDDs for urban dwellers than for rural dwellers. This decrease in HDDs for urban dwellers is normally offset by the increase in CDDs during the summer, which causes more demand for energy-intensive air conditioning.

Landsberg (1981) calculated HDDs and CDDs for multiple cities in the U.S., with measurements taken in two places: urban centers and the surrounding airports. The data show, over the period of 1941 – 1970, an average of 8% more HDDs at the airport than the city centers, and a 12% increase in CDDs in the city centers in the summer (Table 2a; 2b).

Table 2. (a) 1941 – 1970 average for heating degree-day differences[a] between urban and airport stations (Landsberg 1981).

a.

City	Heating degree day		Difference	%
	Urban	Airport		
Los Angeles, CA	692	1011	319	46
Charleston, SC	1078	1192	114	6
Baltimore, MD	2278	2627	349	15
Washington, DC[b]	2339	2467	128	6
St. Louis, MO	2492	2639	147	6
Seattle, WA	2493	2881	388	16
Kansas City, MO	2641	2867	226	9
New York, NY	2693	(2727)[c] 2880	187	7
Denver, CO	3058	3342	284	9
Chicago, IL	3371	(3403)[d] 3609	283	7
Detroit, MI	3460	3556	96	3
Albany, NY	3552	3827	275	8

[a] Base 18°C.
[b] In Washington, D.C., the National Airport is close to the middle of the metropolitan heat island. It was therefore chosen as the "urban" station. For comparison, the station College Park in suburban Maryland at the edge of the urban heat island is given in the "Airport" column.
[c] La Guardia Airport.
[d] Midway Airport.

(b) 1941 – 1970 average for cooling degree day differences[a] between urban and airport stations (Landsberg 1981)

b.

City	Cooling degree days Urban	Airport	Difference	%
Seattle, WA	111	72	39	35
Albany, NY	366	321	45	12
Detroit, MI	416	366	50	12
Denver, CO	416	350	66	16
Chicago, IL	463	(518)[b] 372	91	20
New York, NY	598	(586)[c] 482	116	11
Los Angeles, CA	663	344	319	48
Washington, DC	792	650	142	18
Baltimore, MD	835	620	215	14
Kansas City, MO	857	795	62	7
St. Louis, MO	918	826	92	6
Charleston, SC	1318	1164	154	7

[a] Base 18°C.
[b] Midway Airport.
[c] La Guardia Airport.

b. *Synoptic Fluctuations of the Urban Heat Island*

Wind is by far the most influential synoptic effect determining the magnitude of an UHI. Summers (1964) quantified the change in temperature between urban and rural areas ($\Delta T_{U\text{-}R}$) as a function of five different variables, focusing on the effect of wind:

$$\Delta T_{\mathrm{u-r}} = \left(2r \frac{\partial \Theta}{\partial z} Q_{\mathrm{u}}\right) \Big/ (\rho c_{\mathrm{p}} u)$$

where:

r	- distance from upwind edge of the city to the center
$\delta\theta/\delta z$	- potential temperature θ increase with height z
Q_u	- urban excessive heat per unit area
ρ	- air density
c_p	- specific heat at constant pressure
u	- wind speed

Oke (1976) used Summer's work to test the influence of wind on the UHI in Vancouver, British Columbia (Figure 9). He found that as wind speed approaches 9 meters sec^{-1}, the temperature differential between urban and rural sites ($\Delta T_{U\text{-}R}$) levels off to about 2°C.

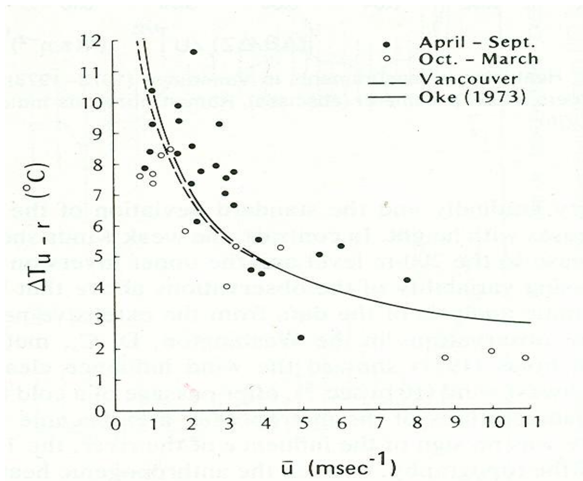

Figure 9. Vancouver UHI intensity ($\Delta T_{U\text{-}R}$), 1 – 3 hours after sunset (Oke 1976).

Atmospheric stability also has the \ability to influence the magnitude of urban warming. Atmospheric stability can be described most simply as the movement of an air parcel within the atmosphere (Carbone 2004). For example, in urban areas intense surface warming will heat an air parcel just above the surface, tending to move that parcel upwards in the atmosphere. Under stable atmospheric conditions, negative buoyant forces (created as the difference in temperature between the ambient air and the air parcel) act on this air parcel as it moves into a cooler, higher-elevation atmosphere, forcing it back down toward the surface. In unstable atmospheric conditions, positive buoyant forces will act on the air parcel and it will continue to rise. In neutral atmospheric conditions, there are no buoyant forces acting on the air parcel, resulting in the parcel remaining in the displaced location. The magnitude of urban warming tends to be higher under stable atmospheric conditions because air parcels become trapped at the surface, allowing for prolonged warming by urban surfaces. In unstable conditions, urban warming is decreased because positive buoyant forces will pull air parcels away from the surface, negating prolonged warming from the urban surfaces. Although there are no buoyant forces under neutral atmospheric conditions, air parcels are still often displaced by wind, which will tend to decrease the effects of urban warming.

Turner class (TC) is a measure of atmospheric stability based on wind speed, cloud cover, and time of day. Turner Classes range from 1-7, with 1 being unstable atmospheric conditions, 4 neutral atmospheric conditions, and 7 stable atmospheric conditions (Panofsky and Dutton 1984). Heisler et al. (2006) found that the average $\Delta T_{U\text{-}R}$ in Baltimore, MD., was 3.7°C with a stable turner class (TC = 7) and only 1.4°C with a neutral turner class (TC = 4). Therefore stable atmospheric conditions resulted in more pronounced UHI measurements.

3. Gradient Analysis

Gradient analysis refers to viewing or describing subjects (plants, humans, surfaces, etc.) in terms of the spatial and temporal environmental gradients that affect species distribution and abundance, and community composition and structure (Kessell 1979). In ecology it can be used to examine the distribution, growth, and abundance of species or biological communities as a function of independently-measured physical, chemical or biotic properties of their environment (Hall and Hall 1998). Explaining spatial variability through gradient analysis is not a new concept. Whittaker (1956) studied the distribution of tree species along an elevation gradient within the Smoky Mountains, U.S., and showed that tree species were each distributed by their independent responses to gradients of environmental conditions and that consequently communities at each elevation are comprised of those species that grow well there. Kessell (1977; 1979) furthered this analysis by recording variation in species as a function of two variables: elevation and soil moisture level, which he determined using topographic position.

The concept of gradient analysis can be applied to the study of ecosystems along urban-rural gradients to explicitly examine the impact of humans on natural ecosystems (McDonnell and Pickett 1990). For instance, the influence of the UHI on the natural ecosystem processes of Puerto Rico, and the extent to which these ecosystem processes can be influenced, is easily quantifiable using urban-rural gradients (McDonnell and Pickett 1990), and is one of the goals of my work.

Recent work within the LEF in Puerto Rico has analyzed tree distributions, invertebrate species distributions, forest metabolic rates, and cloud formation as a function of elevation (Aide et al. 1996; March et al. 2000; March et al. 2002; Harris 2006, Wu et al. 2006[a]). The focus of my work is integrating the elevational temperature gradient within the LEF with the urban-rural temperature gradient in order to examine the potential effects of the San Juan UHI on the LEF.

a. *Elevational Gradient Research within the Luquillo Experimental Forest (LEF)*[1]

Many biotic and abiotic processes fluctuate based on elevation within the LEF. Records from weather stations located within the LEF indicate a strong gradient in annual rainfall with elevation (Brown et al. 1983). Rainfall increases with elevation from 245

[1] section taken, in part, from "*Factors Influencing the Changing Climate of the Luquillo Mountains, Puerto Rico", tentative title, working book chapter, authors: Robert Waide, David J.R. Murphy*

cm/year at lower elevations to over 400 cm yr^{-1} at 700 meter elevation. Rainfall and cloud formation within the LEF are dependent upon a process called orographic uplift. As a rising air parcel passes over a mountain, it will cool according to a specific adiabatic lapse rate dependent on atmospheric moisture, and if the air parcel cools to the dew point, orographic cloud formation occurs (Stull 2000; Carbone 2004). To understand this phenomenon in Puerto Rico better Wu et al. (2006a; 2006b) developed general linear models to predict cloud cover in the LEF based on three independent topographic variables: slope, aspect, and the difference between elevation and the lifting condensation level (LCL).

This is of particular importance to this study because the elevation at which the lifting condensation level forms is driven by the difference in ambient temperature and dew point temperature (Stull 2000; Carbone 2004). The presence of a pronounced and extensive UHI will effectively raise the ambient temperature, and could potentially force orographic cloud formation to occur higher in the atmosphere. The average elevation of cloud formation, as reported by Wu et al. (2006), is 600 meters. This is similar to the findings of Odum (1970), who reported that cloud formation through the years of 1963 – 1966 occurred at elevations of 350 meters before dawn and 700 meters by midday. I calculate that an average temperature change of only 2.4°C would raise the lifting condensation level to the peak of the Luquillo Mountains, assuming an average adiabatic lapse rate of -0.65°C 100 $meters^{-1}$. This has the potential to disrupt cloud formation, thereby possibly reducing freshwater provision for the SJMA, and causing large disruptions to the ecosystem of the Luquillo Mountains.

Long-term temperature data are more limited than rainfall data. They indicate a decline in both the mean and range of monthly temperatures with elevation. Relative humidity decreases similarly. Wind velocity is greatest at higher elevation sites. Wind direction is generally from the northeast at high elevations but tends to be from the southeast at lower elevation stations (Brown et al. 1983). Harris (2006) tested and supported the hypothesis developed by Odum and Pinkerton (1955) that there is a tradeoff between rate and efficiency given the climatic variation along the elevation gradient within the LEF. The maximum useful energy capture (i.e. net primary productivity) is at the mid-elevations, and not the top or bottom of the mountains.

b. Urban Heat Island Studies Using Urban-Rural Gradients

Mitchell (1961), Chandler (1965), Landsberg (1981), and Summers (1984), determined the magnitude of urban warming by comparing measurements from an urban area to a rural area (see section 2.a). They defined urban areas generally as city centers, or as areas where impervious surfaces dominate the landscape. Rural areas are generally defined as outside city limits, or as areas where vegetation dominates the landscape.

An alternative perspective is to use the concept of urban-rural gradient analysis to study UHIs. McDonnell and Picket (1990) defined the urban-rural gradient paradigm saying: "environmental variation is ordered in space, and that spatial environmental patterns govern the corresponding structure and function of ecological systems, be they populations, communities, or ecosystems." Although this concept was not established formally until 1990, many researchers had already been implementing this paradigm to study UHIs. For example, Oke (1973) mounted a thermistor sensor on automobiles and drove across Southeastern Canada to track temperature differences from urban to rural areas ($\Delta T_{U\text{-}R}$), i.e. tracking temperature variations along the existing environmental patterns of urbanization. He found that urban warming was related to the inverse of the square root of the regional wind speed and the logarithm of the population for each town, shown by the equation:

$$\text{Log } \Delta T_{U\text{-}R} = 0.27 \log P - 0.56 \log \bar{u}^{1/2} - 0.61$$

Where:

P = population

ū = regional wind speed

Oke further refined this equation to show that the magnitude of urban warming along the mobile transects was roughly proportional to the fourth root of the population, according to the equation:

$$\Delta T_{U\text{-}R} = P^{0.27} / 4.04\, \bar{u}^{0.56} \approx P^{1/4} / 4\, \bar{u}^{1/2}$$

Where:

P = population

ū = regional wind speed

This work was expanded in recent years by Comrie (2000), who integrated Oke's moving transect approach with stationary sensors to map the influence of wind on the magnitude of the UHI in Tucson, Arizona. He found that katabatic winds flowing off local mountains created numerous cold pockets within the urban and rural areas. He also observed that urban areas had temperatures ~2°C warmer than their rural upwind counterparts. Morris et al. (2001) studied meteorological station data over a twenty year period in Melbourne, Australia, to derive a relation between wind speed, cloud cover, and UHI intensity. Twenty year data trends revealed an overall average UHI effect of ~1.13°C, with seasonal variations of ~1.29°C in the summer and ~0.98°C in the winter. They found that the UHI effect in Melbourne was proportional to the inverse of the third root of the wind speed. The most pronounced UHIs were observed during clear to nearly-clear sky evenings, with little or no wind.

Other recent studies used a combination of fixed-stations and mobile transects to study the magnitude and geographic range of UHIs. Hawkins et al. (2004) used fixed stations to study the effects of surface-cover in rural landscapes on temperature. They found significant differences (~3.4°C) in the calculation of the UHI (ΔT_{U-R}) depending on which surface type was used to represent the rural landscape, where the smallest UHI to the largest UHI were as follows: hardpan dirt, cultivated vegetation (corn, peach trees, squash, broccoli, cauliflower, and cabbage), and a mowed grass field.

Fast et al. (2005) used a series of 40 fixed stations along an urban-rural gradient in Phoenix, Arizona to calculate the spatial distribution of the UHI and to map a pseudo-vertical temperature profile. Pseudo-vertical temperature profile is defined generally as using ground-based data collection along naturally occurring topographic changes in order to attain estimations of temperature variability with elevation. The stations in this study extended from downtown Phoenix to the surrounding rural areas, including the local mountains. Fast et al. (2005) produced the pseudo-vertical temperature profile using in situ temperature data-loggers placed upon a steep slope of a nearby mountain. The pseudo-vertical profile measurement was validated against radiosonde measurements taken via weather balloons. The average temperature difference (pseudo-vertical – radiosonde) calculated during validation was less than ~2°C. Pseudo-vertical temperature measurements were more accurate before sunrise and after sunset, and less accurate during mid-day hours. Hedquist and Brazel (2006) used a combination of fixed stations and moving transects to study change in temperature between urban, residential neighborhoods, and rural landscapes, also in Phoenix, Arizona. Their data revealed an average urban-rural ($\Delta T_{U\text{-}R}$) temperature difference of ~7°C and an urban-residential neighborhood ($\Delta T_{U\text{-}RES}$) temperature difference of ~3°C.

Oke's seminal work in 1973 served as the foundation for UHI studies, however research on this issue has been undertaken in only a few cities within North America, for example, but not limited to: Phoenix, Tucson, Atlanta, Baltimore and Montreal. Each of these cities creates its own UHI that has different periodic and synoptic fluctuations based on the topographic surroundings, type of vegetation, urban structure etc. My study will apply some of the methodologies developed in these studies to the coastal-tropical city of San Juan, Puerto Rico.

Gonzalez et al. (2005) and Velazquez-Lozada et al. (2006) were the first to measure the UHI in San Juan, Puerto Rico. Gonzalez et al. used a combination of in situ surface data and Airborne Thermal and Land Applications Sensor (ATLAS) data during February, 2004 to study the San Juan UHI. Their results show the existence of a late morning peak in the UHI. This finding is contrary to much of the literature on UHIs that report the peak UHI during the evening hours (Chandler 1965; Oke and East 1971; Landsberg 1981). Gonzalez et al. speculate that the late morning peak is due to low thermal storage caused by a lack of high rise buildings, as well as the ability of the UHI to dominate the sea breeze effect, which under normal conditions, would refresh the coastal areas with cool sea breezes during the day. They also report that impervious surfaces had diel temperature fluctuations of 25°C, while vegetation surfaces had fluctuations around 10°C.

Velazquez-Lozada et al. (2006) used a combination of 4 co-op stations and a Regional Atmospheric Model System (RAMS) to assess the magnitude of the UHI created by San Juan and its impacts on regional climate. They found that San Juan has been warming at rate of 0.06°C yr^{-1} over the last 40 years, and predicted that the UHI in the SJMA in 2050 may be as much as 8°C warmer than surrounding rural areas. RAMS simulations showed that the interaction of the UHI and the atmosphere resulted in large sensible heat fluxes between the upper and lower atmosphere.

In this study I extend the work of Gonzalez et al. (2005) and Velazuez-Lozada et al. (2006) by assessing quantitatively the UHI created by the city of San Juan, using both in situ fixed-stations and a series of mobile transects. I will then use these data to explore the effect of land-cover and wind on UHI formation.

4. Modeling in Puerto Rico

Simulations are defined by Odum and Pinkerton (1955) as "successive calculations of the quantities in the storages as they change with inflows and outflows." I believe that simulation modeling will be important to my proposed work, so it is important to review how simulation modeling has been used previously in Puerto Rico. Recently, simulations were used to describe both the forest and urban ecosystems in Puerto Rico. Wu et al. (2006a; 2006b) used simulation models to predict cloud cover, evapotranspiration, and steam flow within the LEF in Puerto Rico, based on aspect, slope, and lifting condensation level. Harris (2006) used simulation models to assess ecosystem level energy costs and gains along an elevational gradient within the LEF. Chen (2006) initiated the empirical move "down the mountain" by simulating the net energy balance for the entire San Juan metropolitan area. I will model the geographic expansion of the UHI in the future based on existing rates of urbanization within Puerto Rico. From this analysis I hope to determine whether or not the geographic range of the urban heat island has reached or will reach the Luquillo Mountains. I hope that my work will add to the work reported here and, if useful information is found, might focus urban planning on design solutions that minimize the UHI effect

References

Achard, F., H. D. Eva, H.-J. Stibig, P. Mayaux, J. Gallego, T. Richards, and J.-P. Malingreau, 2002: Determination of Deforestation Rates of the World's Humid Tropical Forests. *Science*, **297,** 999-1002.

Aide, T. M., J. K. Zimmerman, L. Herrera, M. Rosario, and M. Serrano, 1995: Forest recovery in abandoned tropical pastures in Puerto Rico. *Forest and Ecology Management*, **77,** 77-86.

Aide, T. M., J. K. Zimmerman, M. Rosario, and H. Marcano, 1996: Forest recovery in abandoned cattle pastures along an elevation gradient in northeastern Puerto Rico. *Biotropica*, **28,** 537 - 548.

Akbari, H., Y. J. Huang, P. Martien, L. Rainer, A. H. Rosenfeld, and H. Taha, 1988: The impact of summer heat islands on cooling energy consumption and CO_2 emissions. *CONF-9708168*, Lawrence Berkeley National Laboratory.

Akbari, H., M. Pomerantz, and H. Taha, 2001: Cool surfaces and shade trees to reduce energy use and improve air quality in urban areas. *Solar Energy*, **70,** 295 - 310.

Bounoua, L., R. S. DeFries, M. L. Imhoff, and M. K. Steininger, 2004: Land use and local climate: a case study near Santa Cruz, Bolivia. *Meteorology and Atmospheric Physics*, **86,** 73.

Brown, S., A. E. Lugo, S. Silander, and J. Leigel, 1983: Research history and opportunities in the Luquillo Experimental Forest. Southern Forest Experimental Station, New Orleans, Louisiana. United States Forest Service

Carbone, G., 2004: *Exercises for Weather and Climate*. Fifth ed. Pearson Education, Inc.

Chandler, T. J., 1965: *The Climate of London*. Hutchinson.

Chen, A., 2006: Meteorological Changes along the Rural-Urban Gradient in Eastern Puerto Rico, Master's Thesis, Environmental and Forest Biology, SUNY - College of Environmental Science and Forestry.

Comrie, A. C., 2000: Mapping a wind-modified urban heat island in Tucson, Arizona (with comments on integrating research and undergraduate learning). *Bulletin of the American Meteorological Society*, **81,** 2417-2431.

Douglas, I., 1983: The Energy Balance of the City. *The Urban Environment*, Arnold.

Durland, W. D., 1929: Forest regeneration in Puerto Rico. *Economic Geography*, **5,** 369 - 381.

Fast, J. D., J. C. Torcolini, and R. Redman, 2005: Pseudovertical temperature profiles and the urban heat island measured by a temperature datalogger network in Phoenix, Arizona. *Journal of Applied Meteorology*, **44,** 3-13.

Franco, P. A., P. L. Weaver, and S. Eggen-McIntosh, 1997: Forest resources of Puerto Rico, 1990. United States Department of Agriculture, Forest Service, Southern Research Station

Gill, T., 1931: *Tropical forests of the Caribbean*. The Read-Taylor Co.

Gomez, L. and M. Ballestero, 1980: *Vida y Cultura Precolombina de Puerto Rico. Editorial Cultural*.

Gonzalez, J., Jeffery C. Luvall, Douglas Rickman, Daniel Corazamy, Ana Picon, Eric Harmsen, Hamed Parsiani, Ramon E. Vasquez, Nezario Ramirez, Robin Williams, Robert W. Waide, and Craig A. Tepley, 2005: Urban heat islands developing in coastal tropical cities. *EOS, Transactions, American Geophysical Union*, **86,** 397.

Hall, M. H. P. and C. A. S. Hall, 1998: Using gradient analysis to determine biophysical constraints to economic return on investment in the Costa Rican agricultural sector. *Advances in Energy Studies: Energy Flows in Ecology and Economy*, Musis, Rome.

Hall, M. H. P. and D. B. Farge, 2003: Modeled climate -induced glacier change in Glacier National Park, 1850 - 2100. *Bioscience*, **53,** 131-140.

Harris, N. L., 2006: The carbon balance of a tropical forested ecosystem along an elevational gradient in the Luquillo Mountains, Puerto Rico: an empirical and modeling study scaled from leaves to landscapes, Ph.D. Dissertation, Environmental and Forest Biology, SUNY - College of Environmental Science and Forestry.

Hawkins, T. W., A. J. Brazel, W. L. Stefanov, W. Bigler, and E. M. Saffell, 2004: The role of rural variability in urban heat island determination for Phoenix, Arizona. *Journal of Applied Meteorology*, **43,** 476-486.

Hedquist, B. C. and A. J. Brazel, 2006: Urban, residential, and rural climate comparisons from mobile transects and fixed stations: Phoenix, Arizona. *Journal of the Arizona-Nevada Academy of Science*, **38,** 77-87.

Heisler, G., J. Walton, S. Grimmond, R. Pouyat, K. Belt, D. Nowak, I. Yesilonis, and J. Hom, 2006: Land-cover influences on air temperature in and near Baltimore, MD.

International Conference on Urban Environment, Gotheburg, Sweden.

Helmer, E. H. and B. Ruefenacht, 2005: Cloud-free satellite image mosaics with regression trees and histogram matching. *Photogrammetric Engineering and Remote Sensing*, **71,** 1079–1089.

Johnston, S., 2005: The green development in Chicago. *Economic Development Journal*, **4,** 12-19.

Kessell, S. R., 1977: Gradient Modeling: A new approach to fire modeling and resource management. *Ecosystem modeling in theory and practice*, C. A. S. Hall and J. W. Day, Eds., Wiley, 575-605.

Kessell, S. R., 1979: *Gradient Modeling: resource and fire management*. Springer-Verlag.

Koenig, N., 1953: A comprehensive agricultural program for Puerto Rico. United States Department of Agriculture and Commonwealth of Puerto Rico

Landsberg, H. E., 1981: *The Urban Climate*. Vol. 28, *International Geophysics Series*, Academic Press.

Landsberg, H. E. and D. A. Brush, 1980: Some observations of the Baltimore, Md., heat island. *Inst. Phys. Sci. Technol. Tech. Note*, University of Maryland.

Lutgens, F. K. and E. J. Tarbuck, 1982: *The Atmosphere*. Prentice-Hall.

March, J. G., J. P. Benstead, C. M. Pringle, and M. W. Ruebel, 2000: Linking shrimp assemblages with rates of detrital processing along an elevational gradient in a tropical stream. *Canadian Journal of Fisheries and Aquatic Sciences*, **58,** 470 - 478.

March, J. G., C. M. Pringle, M. J. Townsend, and A. I. Wilson, 2002: Effects of freshwater shrimp assemblages on benthic communities along an altitudinal gradient of a tropical island stream. *Freshwater Biology*, **47,** 377 - 390.

McDonnell, M. J. and S. T. A. Pickett, 1990: Ecosystem structure and function along urban-rural gradients: an unexploited opportunity for ecology. *Ecology*, **71,** 1232-1237.

McPherson, E. G., D. Nowak, G. Heisler, S. Grimmond, C. Souch, R. Grant, and R. Rowntree, 1997: Quantifying urban forest structure, function, and value: the Chicago Urban Forest Climate Project. *Urban Ecosystems*, **1,** 49-61.

Microsoft (2005). Microsoft Streets and Trips, Microsoft.

Millan, M. M., M. J. Estrela, and M. J. Sanz, 2005: Climatic feedbacks and desertification: The Mediterranean Model. *Journal of Climate*, **18,** 684-701.

Mitchell, J. M., 1961: The temperature of cities. *Weatherwise*, **14,** 224-229.

Morris, C. J. G., I. Simmonds, and N. Plummer, 2001: Quantification of the influences of wind and cloud on the nocturnal urban heat island of a large city. *Journal of Applied Meteorology*, **40,** 169-182.

Nowak, D. J. and J. T. Walton, 2005: Projected urban growth (2000 - 2050) and its estimated impact on the U.S. Forest Resource. *Journal of Forestry*, **103,** 383-389.

Odum, H. T. and R. C. Pinkerton, 1955: Time's speed regulator, the optimum efficiency for maximum output in physical and biological systems. *American Scientist*, **43**.

Oke, T. R. and C. East, 1971: The urban boundary layer in Montreal. *Boundary Layer Meteorology*, **1,** 411-437.

Oke, T. R., 1973: City size and the urban heat island. *Atmospheric Environment*, **7,** 769-779.

Oke, T. R., 1976: The distinction between canopy and boundary layer urban heat islands. *Atmosphere*, **14,** 268-277.

Panofsky, H. A. and J. A. Dutton, 1984: *Atomspheric Turbulence*. John Wiley, 397 pp.

Quale, R. G. and H. F. Diaz, 1979: Heating degree day data applied to residential heating energy consumption. *Journal of Applied Meteorology*, **19,** 241 - 246.

Ricardo, D., 1911: *On the Principles of the Political Economy and Taxation*. J.M. Dent and Sons, Ltd.

Stull, R. B., 2000: *Meteorology: for scientists and engineers*. Second ed. Brooks/Cole.

Summers, P. W., 1964: An urban ventilation model applied to Montreal, Ph.D. Dissertation, McGill University.

UN-POP, 2003: World Population Prospects: The 2003 Revision. Population Division of the Department of Economic and Social Affairs of the United Nations Secretariat. http://esa.un.org/unpp

UN-POP, 2004: World Population Prospects: The 2004 Revision. Population Division of the Department of Economic and Social Affairs of the United Nations Secretariat. http://esa.un.org/unpp

van der Molen, M. K., 2002: *Meteorological Impacts of Land Use Change in the Maritime Tropics*. Academisch Proefschrift.

Velazquez-Lozada, A., J. Gonzalez, and A. Winter, 2006: Urban heat island effect analysis for San Juan, Puerto Rico. *Atmospheric Environment*, **40,** 1731-1741.

Wadsworth, F., 1950: Notes on the climax forests of Puerto Rico and their destruction and conservation prior to 1900. *Caribbean Forester*, **11,** 38-47.

Whittaker, R. H., 1956: Vegetation of the Great Smoky Mountains. *Ecological Monographs*, **26,** 1-80.

World Resources Institute. (2006). www.earthtrends.org. Washington, D.C.

Wu, W., C. Hall, and L. Zhang, 2006a: Predicting the temporal and spatial probability of orographic cloud cover in the Luquillo Experimental Forest in Puerto Rico using generalized linear (mixed) models. *Ecological Modeling*, **192,** 473-498.

Wu, W., C. A. S. Hall, F. N. Scatena, and L. J. Quackenbush, 2006b: Spatial modeling of evapotranspiration in the Luquillo Experimental Forest of Puerto Rico using remotely-sensed data. *Journal of Hydrology*, **328,** 733-752.

The Relation between Land-Cover and the Urban Heat Island in Northeastern Puerto Rico

David J. R. Murphy

State University of New York – College of Environmental Science and Forestry,
1 Forestry Drive, Syracuse, New York, 13210
djmurp03@syr.edu

Abstract. Population growth and industrialization are causing rapid urbanization throughout the tropics, resulting in elevated temperatures within urban areas, a phenomenon known as the Urban Heat Island (UHI). One such example is the city of San Juan, Puerto Rico, where intense urbanization has caused the formation of a pronounced UHI. My objective in this study is to quantify the UHI created by the San Juan Metropolitan Area over space and time.

I collected temperature data using mobile transects and fixed-station transects spanning along several urban-rural gradients to show the UHI created by San Juan. I also used this data to examine the relation between average temperature and upwind vegetation. Regression analysis of upwind vegetation vs. average temperature was used to predict temperature based on land-cover change over time.

My data shows the existence of a nocturnal UHI, with nighttime urban-rural temperature differences (ΔT_{U-R}) of up to 3.02°C. Comparisons of diel temperature trends at urban, grassland, and forested sites indicate that canopy cover is needed to reduce daytime UHI effects. My data also shows that the UHI is encroaching on the Luquillo Mountains which may alter the water supply for San Juan. Temperature was predicted best ($r^2 = 0.94$) by vegetation in southeasterly upwind directions within 180 meters of the sensor, and under a 'business as usual' urbanization scenario, over 140 km^2 of land that showed now signs of UHI in 2000 will have a UHI between +0.4°C - +1.55°C on average by 2050. Furthermore, over 130 km^2 of land area with a UHI between +0.4°C and +1.4°C in 2000 will have a UHI of +1.55°C on average by 2050.

Keywords: Urban Heat Islands, urban-rural gradients, land-cover

1. Introduction

In 2007, global urban populations are projected to outnumber global rural populations for the first time in history, with the fastest urban growth rates in the developing nations of the world (UN-POP 2004). Puerto Rico is a prime example of this trend, as industrialization and economic development over the past 50 years have resulted in rapid urbanization. Today, over 90% of the Puerto Rican population lives within urban areas (World Resources Institute 2006), the largest of which is the San Juan Metropolitan Area (SJMA).

Urban populations make large demands on ecosystem services of all varieties, not the least of which is the provision of an adequate freshwater supply (Jansson et al. 1999). The SJMA receives much of its freshwater from the Luquillo Mountains, a large forested area located 17 kilometers to the east (Figure 1). There is new concern about a 16% decrease in overall precipitation trends within Puerto Rico during the 20th century (van der Molen 2002), and that three of the top ten driest years in the past century were recorded in the 1990's (Larsen 2000).

It is now fairly well known that global climate change may result in precipitation shifts, causing some areas of the planet to become drier and some areas to become wetter (Millan et al. 2005). A growing body of evidence suggests, however, that urbanization may affect regional climates more than the changes predicted by the influence of global climate change (Hulme and Viner 1995; Scatena 1998a; Brazel et al. 2000). Therefore research efforts should focus not only on global climate change, but also on the regional climatic effects of urbanization, especially the effects of Urban Heat Islands (UHIs).

The UHI is a phenomenon in which urban areas have warmer temperatures than surrounding suburban or rural areas within the same locale (Douglas 1983; Stull 2000; Carbone 2004). Impervious surfaces common to urban areas such as concrete, asphalt, and brick retain radiation throughout the day and reemit it during the night, increasing the sensible temperature during the evening hours. This effect distorts the natural sun-earth radiation balance, and is the ultimate forcing behind UHI formation (Douglas 1983; Stull 2000; Carbone 2004). The specific amount of radiation retained, and the rate at which it is released depends on the physical characteristics of the surface material. However, the degree to which radiation released by surfaces within an urban environment affects sensible air temperature is often not easy to measure, mainly due to the presence of wind.

Wind is often cited as the most important meteorological factor influencing the formation of the UHI (Oke 1976; Landsberg 1981; Gonzalez 2005). This is due in part to the natural process of evaporative cooling, which is accelerated by the presence of wind, and is often utilized in urban areas to mitigate warming through projects such as 'green roofs'. In Puerto Rico, Odum et al. (1970) and Brown (1983) found that the prevailing wind direction is from the north-east at mid- to high elevations (> 300 meters above sea level), but generally from the east-southeast at low elevations (< 300 meters above sea level). However, the extent to which the prevailing wind pattern influences urban warming in San Juan is currently unknown, and will be analyzed in this paper.

Just as wind plays an important role in the formation of the UHI, the UHI itself plays an important role in the formation of clouds, and ultimately the location and amount of precipitation (Rosenfeld 2000; Dixon and Mote 2003; Millan et al. 2005).

Since most of the fresh water provision for the SJMA comes from the Luquillo Mountains, a shift in cloud level driven by spreading UHI, especially towards the Luquillo Mountains, may result in additional water shortages.

Most of the precipitation within the Luquillo Mountains is the result of orographic uplift (Daly et al. 2003). Orographic uplift is a process by which cloud formation occurs as a result of air masses rising along the slopes of mountains, cooling adiabatically to the lifting condensation level, where they form clouds or rain (Stull 2000; Carbone 2004). This process can be altered by the existence of UHIs. Scatena (1998b) reports that the influence of land-cover change on regional climates throughout Puerto Rico, e.g. UHIs, can effect species distribution and rainfall patterns within the Luquillo Mountains by altering the altitude of cloud formation, i.e. the lifting condensation level. The average elevation of cloud formation, as reported by Wu et al. (2006), is 600 meters. This lies within the range reported by Odum et al. (1970), who found that cloud formation through the years of 1963 – 1966 occurred at elevations of 350 meters before dawn and 700 meters by midday. I calculate that an average temperature change of only 2.4°C would raise the lifting condensation level to the peak of the Luquillo Mountains, when using an adiabatic lapse rate of -0.65°C 100 meters^{-1}. This would disrupt cloud formation, thereby limiting freshwater provision for the SJMA, and cause enormous disruption to the ecosystem of the Luquillo Mountains.

In recent studies, Gonzalez et al. (2005) and Velazquez-Lozada et al. (2006) have shown both the existence of a pronounced UHI in San Juan and also the potential impacts of the UHI on precipitation downwind of the city. However, these studies have not focused on the influence of prevailing wind patterns on temperature or the potential impacts of the UHI on the lifting condensation level within the Luquillo Mountains. Gonzalez et al. (2005) used a combination of data collected by in situ temperature sensors and Airborne Thermal and Land Applications Sensor (ATLAS) data during February of 2004 to study the San Juan UHI. Their results show the existence of a late morning peak in the UHI. This finding is contrary to much of the literature on UHIs that report the peak UHI during the evening hours (Chandler 1965; Oke and East 1971; Landsberg 1981). Gonzalez et al. speculate that the late morning peak is due to low thermal storage caused by a lack of high rise buildings, as well as the ability of the UHI to dominate the sea breeze effect, which under normal conditions, would refresh the coastal areas with cool sea breezes during the day. They also report that impervious surfaces had diel temperature fluctuations of 25°C, while vegetated surfaces had fluctuations of around 10°C.

Velazquez-Lozada et al. (2006) used a combination of 4 co-op stations and a computer simulation model called the Regional Atmospheric Model System (RAMS) to assess the magnitude of the UHI created by the SJMA and its influence on regional climate. They reported that San Juan has been warming at rate of 0.06°C year^{-1} over the last 40 years, and predicted that the UHI in 2050 created by the SJMA may be as much as 8°C warmer than surrounding rural areas. RAMS simulations showed that the interaction of the UHI and the atmosphere resulted in large fluxes of sensible heat between the upper and lower atmosphere.

As development continues in Puerto Rico, forests and grasslands are being converted to impervious cover, changing the magnitude and geographic range of the UHI. Using data collection methods developed by Chandler (1965), Oke (1973), Landsberg (1981), Comrie (2000), Hawkins et al. (2004), Fast et al. (2005), Hedquist and Brazel (2006), and Heisler et al. (2006), and some new modeling techniques, I was able to examine the relation between land-cover and the UHI explicitly, and from this I hope to provide a more thorough understanding of the effects that urbanization may impart on the ecosystem services provided by the forest, including the freshwater supply for the SJMA. I applied these methods using the spatial framework of an urban-rural gradient (McDonnell and Pickett 1990). This will allow me to quantify the timing of the peak UHI in the SJMA, explore correlations between urban warming and land-cover, and predict growth of the geographic range of the UHI.

2. Objectives:

My objectives, therefore, are as follows: (1) to quantify the timing of the peak urban heat island created by the San Juan Metropolitan Area, (2) to explore correlations between air temperature and land-cover, (3) to assess the geographic range of the urban heat island created by the San Juan Metropolitan Area, and (4) to predict the growth of the geographic range of the UHI based on a ‘business as usual’ urbanization scenario.

3. Hypotheses:

I hypothesize that: (1) San Juan has a daytime peak in the urban heat island effect; (2) the urban heat island effect decreases as the distance from urban center increases; (3) the urban heat island effect extends to at least the foothills of the Luquillo Mountains; (4) temperature is related to the quantity of vegetation cover upwind.

4. Methods

I employed two methods to capture the variation of UHI over space and time: (a) a fixed-station transect of temperature sensors, and (b) a mobile temperature measurement transect. For the fixed-station transect I installed a network of ten automated Series-8 HOBO Pro-Temp Data Loggers (Onset Corporation; Figure 1), to record temperature measurements along several urban-rural gradients throughout the SJMA. The goal of the fixed-station transect was to establish near-simultaneous temperature measurements along the gradients to assess the timing of the peak UHI and the influence of land-cover on temperature. For the mobile measurements I attached a thermistor-temperature sensor to the roof of a Jeep Cherokee and drove along different routes radiating out from the central business district (CBD) of the SJMA to three different surrounding rural areas. The goal of the mobile data collection was to capture the geographic range of the UHI.

Figure 1. Series-8 HOBO Pro Temp Data Logger produced by the Onset Corporation.

I created a model in Fortran-90 language that calculated from a 30-meter resolution land-cover map of Puerto Rico the amount of vegetation upwind from each HOBO sensor at varying upwind directions and increasing distances. By combining the model output with average temperature data recorded by each HOBO, I was able to correlate temperature with upwind vegetation. I applied this correlation to an urbanization model developed in IDRISI to predict the growth of the geographic range of the UHI into the future.

a. Fixed-Station Transects

In this approach I recorded temperatures along an urban-rural gradient with fixed-stations to study the relation between temperature and land-cover. I defined an urban-rural gradient as a continuum along which the average land-cover at any point changes from less vegetation to more vegetation, i.e. suburban to forested cover, without proceeding necessarily in that order. Due to the logistical difficulties associated with studying an area as large as the SJMA, I chose a smaller urban area to the east that spans a distance of only 5 kilometers (Figure 2a and 2b), and compared diel temperature trends between HOBOs to examine the influence of both local and upwind land-cover on warming during the day and cooling during the night.

1) INSTALLATION

The gradient begins and ends with two rural grassland sites. HOBO 1S, the most northern HOBO, was placed in a landscape dominated by abandoned agricultural fields (Table 1), and HOBO 6S, the most southern HOBO, was placed in a mowed-grassland behind a major shopping center upwind of all development, located in the foothills of the Luquillo Mountains (Figure 2b). The middle of the gradient, HOBO 2S – HOBO 5S, is the most urbanized landscape comprised of one story concrete houses, one large pharmaceutical industry, and major roadways.

Table 1. List of all HOBOs and the predominant local land cover. "S" designates HOBO locations during the "summer" data collection period, and "F" designates HOBO locations during the "fall" data collection period. "A" designates the 'additional' HOBOs used during both the summer and fall data collection periods.

HOBO ID	Local Land-Cover
1S	Abandoned agricultural fields
2S	Urban center
3S	Industrial
4S	Residential
5S	Major road crossing
6S	Mowed-grassland
1A	San Juan central business district (CBD)
2A	Old-growth forest
3A	Grassland/tree/impervious mix
4A	Abandoned agricultural fields
1F	Residential
2F	Residential
3F	Mowed-grassland/trees
4F	Major road crossing
5F	Grassland/tree/impervious mix
6F	Abandoned agricultural fields/trees

a. Northeastern Puerto Rico - Urban Heat Island Study Area

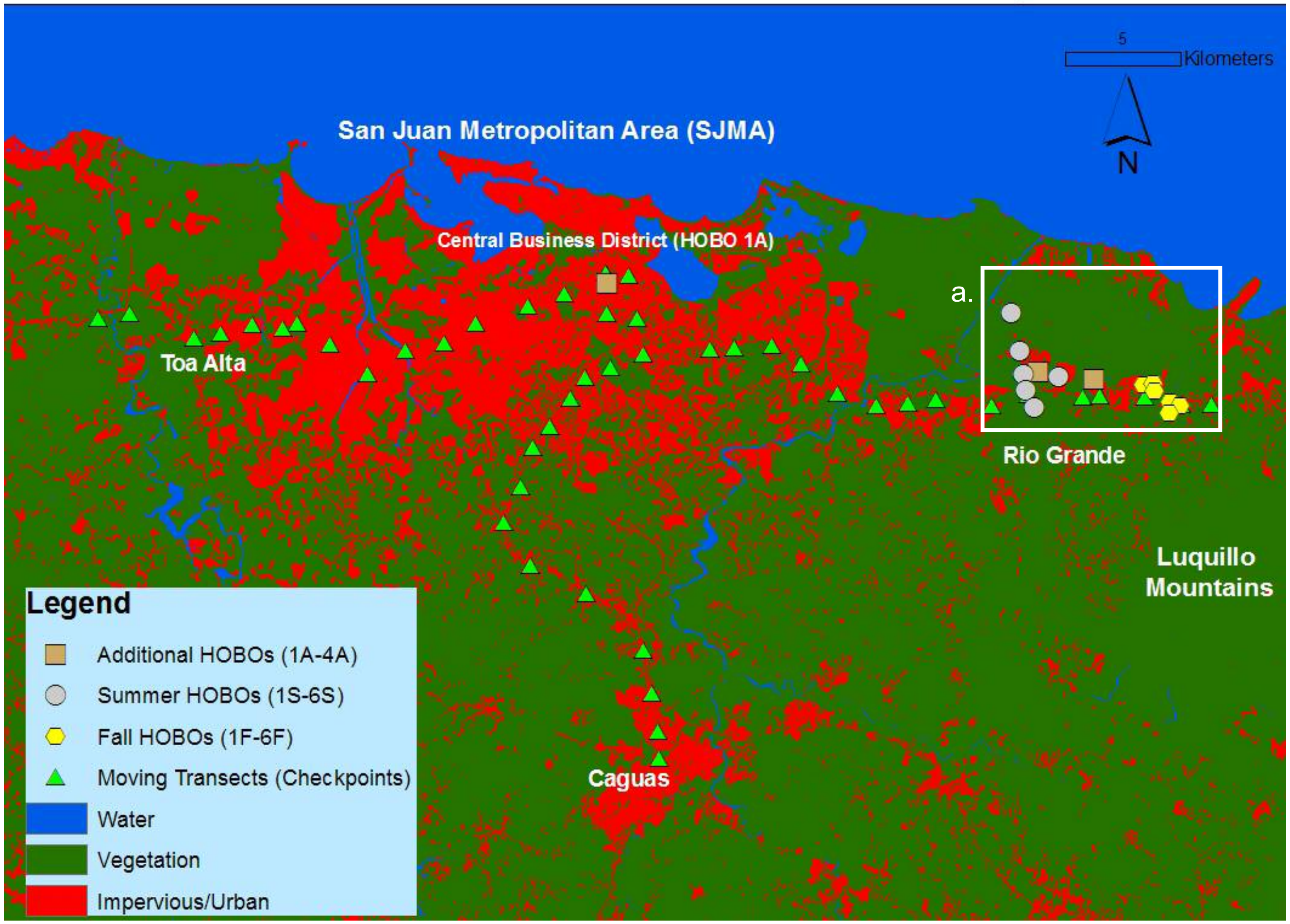

Figure 2a. Land-Cover map of Northeastern Puerto Rico with green triangles labeling checkpoints during the mobile transects. The grey circles, yellow hexagons, and the brown squares mark the locations of the HOBOs.

b.

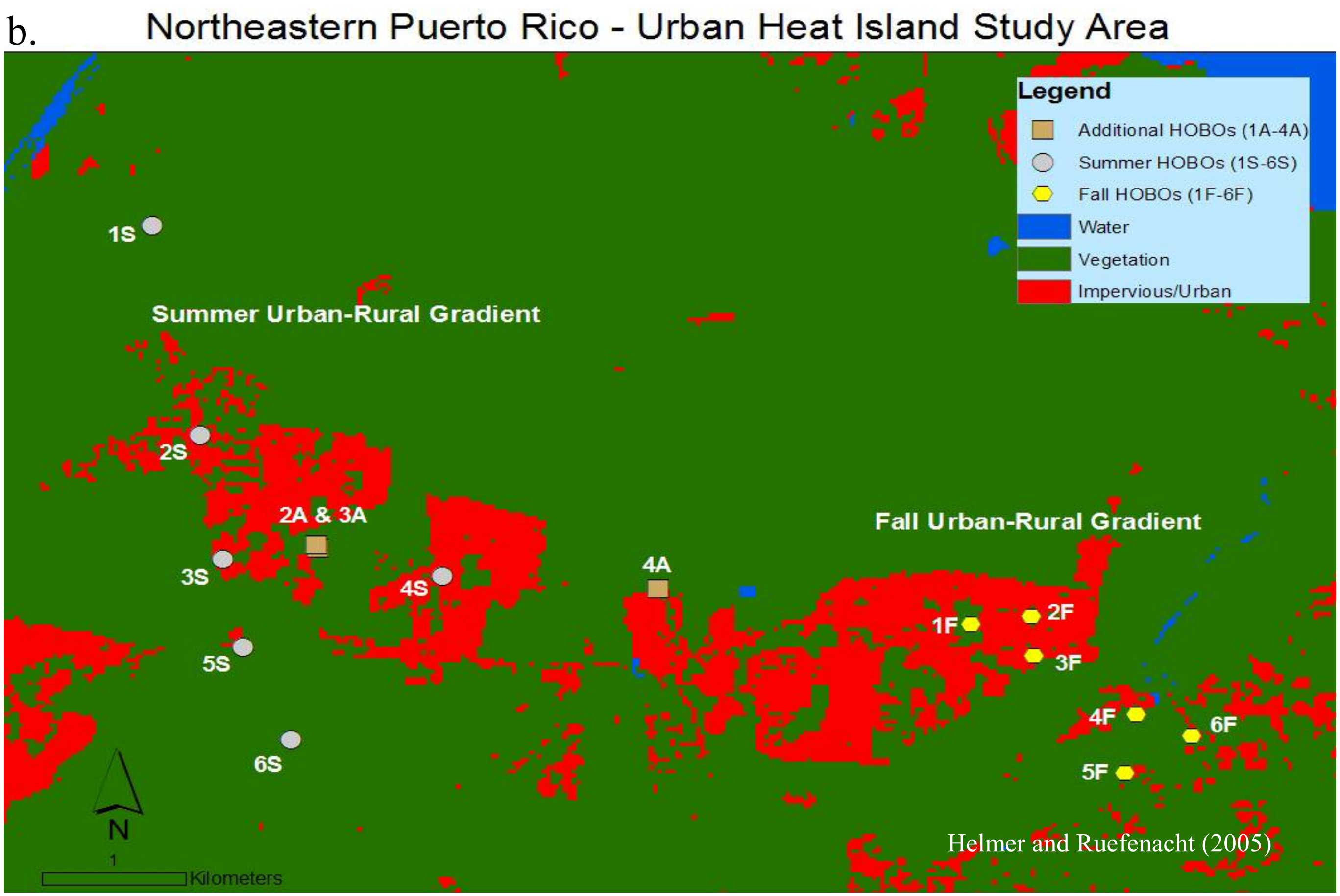

Figure 2b. This is a map of the summer and fall urban-rural gradients, as well as additional HOBOs placed in the field. The grey circles, labeled HOBO 1S – 6S, were moved during the fall and became HOBO 1F – 6F. The “additional HOBOs”, 1A – 4A (A1 shown in Figure 1), remained at the same locations for both the summer and fall data periods.

I placed HOBOs 1A – 4A at four additional locations in order to represent the temperature differences between a highly urbanized area and the surrounding rural areas more fully (Table 1), i.e. in vegetated or urban environments not adequately represented by the other sites. These include: 1A) the central business district (CBD) of the SJMA, which was used to represent the most intensely urbanized area within northeastern Puerto Rico. I used this site to measure the magnitude of the UHI, calculated as the difference in average temperature between the San Juan CBD and other locations along the gradient (ΔT_{CBD-HB}); 2A) an old growth forest, which represents the natural forest ecosystem of Puerto Rico; 3A) the same general location as 2A but in a lightly developed area, comprised of both grasslands and impervious cover. Placing these two HOBOs in the same locale, but with completely different vegetated surroundings made it possible to examine the influence that canopy cover vs. regional development may have on the presence or intensity of the UHI. I placed HOBO 4A in an abandoned agricultural land, upwind of all development, as a control.

In addition to land-cover considerations, I selected installment locations based on 2 criteria: (1) accessibility for downloading data, and (2) the relative security of the site. I attached the HOBO loggers to utility poles along roadways roughly 3 meters above ground level using plastic straps. Each HOBO logger was encased by a Solar Radiation Shield (Onset Corporation) in order to minimize the impacts of direct sunlight on the temperature sensors. I set the data loggers to collect one instantaneous temperature measurement at 5 minute intervals for two collection periods during the summer of 2006, June 26 – July 5, and July 10 – July 20.

During the early fall of 2006 (9/10 – 10/7) I moved six HOBOs (HB1S – HB6S) to new locations, using the same criteria for site selection, identified in Figure 2b as 1F-6F. This second data set increased the spatial coverage of the HOBO data, while also providing a data set for model validation. It should be noted that comparisons between the summer and fall data sets were possible only because of the tropical, and hence more consistent inter-seasonal climatic patterns in Puerto Rico. To verify this for the 2 seasons of collection, I examined monthly climate summaries provided by the National Weather Service, post data-collection, to ensure that there were no major climatic events (i.e. hurricanes, etc.) during the 2 data collection periods.

Before deploying the HOBOs in the field, I performed an inter-HOBO calibration procedure to ensure precision between sensors. Each HOBO was placed inside a climate controlled room for a period of 9 hours recording one instantaneous temperature measurement every minute (n = 540 observations). From this data I calculated 95% tolerance intervals for each of the HOBOs (Table 2), and found significant overlapping between the HOBO measurements, indicating that the HOBO measurements were all close to one another, and that a recalibration of the HOBOs was not needed.

Table 2. Average temperature measurements and tolerance intervals recorded during the calibration period.

HOBO Calibration (n = 540 observations)	
Temperature Average	Tolerance Interval
18.94	18.45 - 19.43
18.84	18.42 - 19.25
18.83	18.46 - 19.20
18.80	18.43 - 19.17
18.79	18.43 - 19.14
18.77	18.42 - 19.12
18.66	18.17 - 19.15
18.65	18.13 - 19.17
18.63	18.26 - 19.00
18.58	18.07 - 19.10
average = 18.75, Standard Deviation = 0.11	

2) AIRSHED DELINEATION AND LAND-COVER

My first analysis of the relation between land-cover and average temperature did not consider wind as an important factor in measuring temperature, but rather analyzed the influence of percent vegetation surrounding the temperature sensor in all directions between 30 and 5000 meters away from the sensor as the predominant influence on average air temperature. This model predicted temperature poorly ($r^2 = 0.003$). Due to the importance of wind mitigation on the magnitude of UHIs, as shown by other UHI researchers (Summers 1964; Oke 1976; Comrie 2000; Morris 2001; Gonzalez et al. 2005), I decided to look upwind from each sensor and analyze the percent vegetation at different angles and distances upwind. To do this I developed a computer model in Fortran-90 language (code available in Appendix A) that calculated the percent of vegetation within a cone-shaped upwind area, termed an “airshed”. The percent vegetation is derived from a year 2000 land-cover map of Puerto Rico (Helmer and Ruefenacht 2005), according to the formula:

$$\textbf{Percent vegetation upwind} = \frac{\textbf{Number of vegetated pixels within upwind airshed}}{\textbf{Total number of pixels within upwind airshed}} * \mathbf{100}$$

The location of each HOBO on the ground was georeferenced using latitude and longitude coordinates and projected to the spatial reference system of the 2000 land cover map, NAD-1927 Lambert Conformal Conic. I calculated percent upwind vegetation for each HOBO site by creating an airshed whose dimensions were determined by azimuth degree and upwind distance. The model analyzed a total of 180 azimuth degrees, from due north to due south, and a maximum of 2520 meters upwind. I divided the azimuth degrees into 18 windows of 10 degrees each, termed “degree window”, and divided the “upwind distance” into 84 intervals of 30 meters each (Figure 3). The model began on a ‘center pixel’, representing the site of the first HOBO, and selected the first of the 18 degree windows (81° – 90°) and the first of the upwind distances (30 meters) from which it formed the airshed. The percent vegetation was calculated for the airshed, and the resulting percentage was assigned to the center pixel. This process was repeated for every HOBO location on the map using the first degree window and the first upwind distance. On the second pass, the model changed to the second upwind distance (60 meters) and calculated the percent vegetation from a 60 meter airshed. Once the model calculated percent vegetation using all 84 upwind distances in degree window 1, it switched to degree window 2 (71° - 80), and the entire process was repeated for all HOBO locations on the map. In total, percent vegetation was calculated using 18 degree windows each with 84 upwind distances, creating 1512 airsheds.

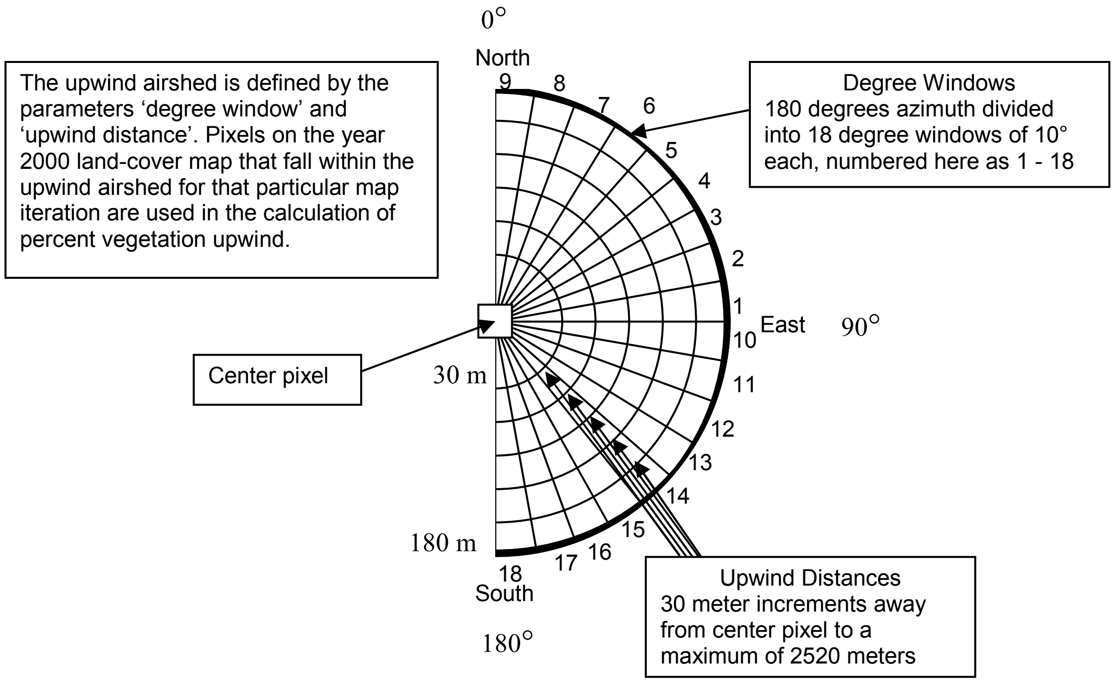

Figure 3. This is a conceptual diagram of the airshed model. The box in the center is called the 'center pixel' and represents the hobo on the ground for which the average vegetation upwind is being calculated. The program starts on degree window 1, the wedge just above 90° east, and calculates the percent vegetation within the upwind wedge using all possible distances upwind from 30 to 2520 meters, at 30 meter intervals. Once this calculation is complete for all distances in degree window 1, the program switches to degree window 2 and repeats the calculation for all distances in degree window 2. Once degree window 9 is reached, which is the most northern facing wedge (1°– 10°), the program will switch to degree window 10 and repeat the process for degree windows 10 – 18, ending with the most southern facing wedge (171° - 180°).

3) ANALYSIS OF THE RELATION BETWEEN TEMPERATURE AND LAND-COVER

After each pass of the land-cover map, values for row, column, HOBO name, upwind degree, upwind distance, and percent vegetation for each of the pixels representing HOBOs were written to a text file. I imported this text file into Microsoft Excel and calculated the square of the Pearson Product Moment Correlation Coefficient (r^2) between percent vegetation and average HOBO temperature. The r^2 value can be interpreted as the proportion of the variance in y attributable to the variance in x, and was used to test the hypothesis that the dependent variable (temperature) is explained by the independent variable (percent vegetation) in the upwind direction (H_4). I calculated r^2 values between percent vegetation for each of the 1512 airsheds and average temperature data collected by HOBOs 1S-6S and 1A - 4A during the summer of 2006. All 1512 r^2 values were grouped into 9 classes, each with a range of 0.09, and plotted in a gradient space dimensioned by azimuthal degree on the y-axis and upwind distance on the x-axis. Each different class represents an 'isocorrelation', defined as a group of r^2 values that all fall within the same range. From these 1512 r^2 values, I selected the highest r^2 and fit the data to a linear regression, called the best-fit regression, according to the formula:

$$T = \alpha + \beta x$$

Where:
- T = average temperature
- α = y – intercept
- β = parameter estimate for percent vegetation
- x = percent vegetation

I used this linear regression equation to predict temperature at HOBOs 1F – 6F. By comparing predicted to observed temperatures, I was able to assess the mean absolute error of using an airshed model as a predictor of temperature.

4) URBANIZATION MODEL

I used the GEOMOD module within the IDRISI Kilimanjaro mapping software to predict urbanization to the year 2050 in Northeastern Puerto Rico. I predicted urban growth at decadal intervals starting with the 2000 land-cover map and ending with the year 2050. The 'business as usual' rate of urbanization was determined by subtracting the urban areas in a 1991 land-cover map from the urban areas in the 2000 land-cover map. Using the variables of slope, aspect, distance to roads, distance to urban areas, and distance to coast, derived from the 2000 land-cover map, I created a suitability map in which each pixel has a number representing the suitability of that pixel to change to an urban land-cover from one time step to the next (Pontius 2001). Pixels with higher suitability values were developed first during each time step.

5) CALCULATION OF THE FUTURE URBAN HEAT ISLAND

For each new decade's land-cove map, I repeated the calculation of percent vegetation upwind using the best-fit airshed for every pixel on the new land-cover maps. I converted the percent vegetation maps to temperature maps by multiplying each pixel on each map by the best-fit regression. In order to show geographic growth of the UHI over time, I subtracted the average forest temperature from all pixels on the temperature maps to represent the average temperature departure at each pixel form the natural vegetated ecosystem in Puerto Rico. This statistic is reported as an UHI index.

b. Mobile Measurement Transects

My second data set consisted of temperature measurements collected while driving from the central business district (CBD) of San Juan to areas south, east, and west, to measure the geographic range of the UHI. I repeated the transects at three different time periods during a 24 hour period: 0400 – 0600 hours, 1200 – 1400 hours, and 2000 – 2200 hours (Figure 2a), in order to capture diel fluctuations in the geographic range of the UHI. I used this data along with distance to urban center data to test the hypothesis that the UHI effect decreases as the distance from urban center increases (H_2) and the hypothesis that the UHI effect extends to at least the foothills of the Luquillo Mountains (H_3).

For this analysis, I measured the UHI as the difference in temperature between the CBD of San Juan and all other points along the transect ($\Delta T_{CBD\text{-}Tr}$). I defined distance from urban center as the Euclidean distance, i.e. the shortest linear distance from any point on the map to either the central business district of the SJMA or the central business district of Caguas. I used Caguas in the calculation of distance to urban center because it is also a major city in northeastern, Puerto Rico, but it is not included in the SJMA.

I could drive only one transect on any particular night. Since I was driving these transects on different nights, I needed to ensure that the temperature variations between nights were due to spatial phenomenon associated with the urban-rural gradient rather than differences in climate. For example, comparing data collected during a calm, clear night with that of a windy, cloudy night would show temperature trends affected by climatic differences, and not necessarily geographic temperature trends.

Heisler et al. (2006) correlated the UHI in Baltimore, Maryland with climatic conditions such as cloud cover and wind. They used regression analysis to analyze the UHI as a function of Turner Class, which is an index of atmospheric stability calculated using variables for time of day, cloud cover, cloud height, and wind speed (Panofsky and Dutton, 1984). Based on the findings of Heisler et al. (2006), I used Turner Class indices to gauge climatic differences between evenings. To do this I downloaded data from the National Weather Service and calculated the Turner Class just before I began each transect. I collected data only on nights with Turner Classes of 6 or 7, both of which indicate stable atmospheric conditions.

1) DATA COLLECTION

I used a Campbell Scientific CR21x data logger to collect temperature measurements from a thermistor probe mounted on the top of a Jeep Cherokee. I constructed an L-shaped poly-vinyl chloride (PVC) pipe and attached it to the roof of the Jeep with the shorter arm of the “L” extending vertically away from the roof (Figure 4). The thermistor probe was attached to the top of this extension of the PVC pipe, about one meter from the roof surface and about 2.5 meters above ground level. A cable ran down from the thermistor along the PVC pipe and into the passenger side of the Jeep connecting to the data logger, which was programmed to record temperature measurements at one-minute intervals. In order to ensure that my instruments were precise, I established a secondary thermometer with digital display in an identical fashion as the thermistor probe, and compared visually the digital display to the measurements recorded by the datalogger during the transects. I established checkpoints along each route at roughly 1 km intervals at which point I recorded manually the thermistor temperature from the Campbell Scientific data logger, the digital display temperature, latitude, longitude, and elevation. I drove at speeds less than 50 km/hr and recorded measurements only while the car was moving in order to avoid any effects that may arise while stopped, such as: heat emanating from an idling engine, number and size of surrounding cars, length of stop time, etc.

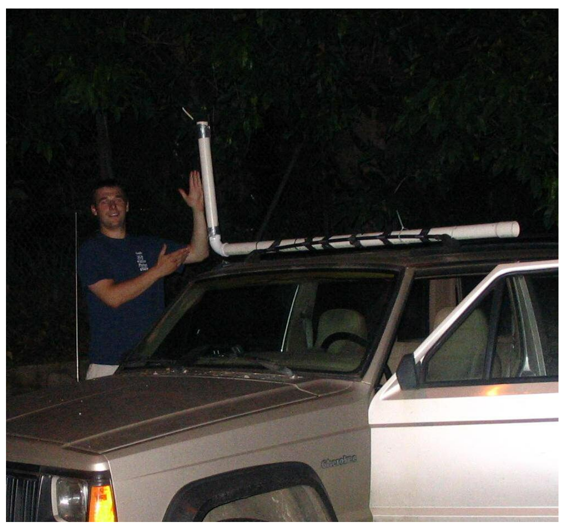

Figure 4. The thermistor probe hangs off the top of the vertical arm of the PVC pipe extending away from the roof. The cable from this probe was run along the vertical arm of the PVC pipe and into the passenger side of the vehicle.

2) ANALYSIS OF THE RELATION BETWEEN TEMPERATURE AND DISTANCE TO URBAN CENTER

I used the distance function within the IDRISI mapping software to create a distance map in which every pixel on the map had one value corresponding to the shortest linear distance to either the central business district of the SJMA or to the central business district of Caguas. I georeferenced the latitude and longitude values for the checkpoints along the mobile transects and assigned them to the pixel on the land-cover map that represents their location on the ground. I overlayed the checkpoint locations on the distance map and then used a cross-tabulation function to retrieve the distance from urban center values for each checkpoint. This data was imported along with the temperature data collected during the moving transects into Excel and linear regression analysis was performed to correlate the dependent variable ($\Delta T_{CBD\text{-}Tr}$) with the independent variable (distance from urban center), according to the formula:

$$\Delta T_{CBD\text{-}Tr} = \alpha + \beta x$$

Where:
$\Delta T_{CBD\text{-}Tr}$ = Change in temperature along the transect
α = y - intercept
β = parameter estimate for distance to urban center
x = distance to urban center

5. Results

a. Fixed-Station Transects

1) URBAN HEAT ISLAND

My results show the existence of a pronounced nocturnal UHI, contrary to my hypothesis that the UHI in the SJMA peaks during the late morning hours (H_1). The UHI was 1.70°C during the early night (1900 – 2359) and 1.81°C during the late night (0000 – 559). Daytime (0600 – 1859) UHI measurements were only 0.93°C (Table 3). Thus the night UHI is twice as great as the day UHI. Individual values of ΔT_{CBD-HB} were highly variable ranging from 0.31°C at the 4S HOBO to 3.02°C at the 6F HOBO.

Table 3. Average temperature difference calculated as urban reference – (individual HOBOs) for all HOBOs along the urban-rural gradient.

UHI (°C) - ΔT_{CBD-HB}				
HOBO	**Local Land Cover**	**Early Night UHI (1900 - 2359)**	**Late Night UHI (0000 - 559)**	**Day UHI (0600 - 1859)**
1S	Abandoned agricultural fields	1.25	1.47	0.97
2S	Urban Center	0.72 (min)	0.83 (min)	0.55 (min)
3S	Industrial	1.32	1.61	0.90
4S	Urban center	0.31	0.64	0.25
5S	Major road crossing	0.78	0.93	0.55
6S	Mowed-grassland	2.44	2.43	0.91
2A	Old-growth forest	2.14	1.86	2.23 (max)
3A	Grassland/tree/impervious mix	1.47	1.44	1.10
4A	Abandoned agricultural fields	2.01	1.76	1.81
1F	Residential100	2.05	2.28	0.80
2F	Residential	1.47	1.74	0.55
3F	Mowed-grassland/trees	1.69	1.90	0.51
4F	Major road crossing	2.09	2.42	0.65
5F	Grassland/tree/impervious mix	3.01 (max)	2.80 (max)	1.02
6F	Abandoned agricultural fields/trees	2.79	3.02	1.20
Average ± Standard Error		**1.70 ± 0.19**	**1.81 ± 0.17**	**0.93 ± 0.13**

The larger ΔT_{CBD-HB} values were calculated between the CBD and stations in open, vegetated areas, not forested areas. For example, HOBO 6S, located in a mowed grass field behind a major shopping center at the foothills of the Luquillo Mountains, was only 0.91°C cooler than the CBD of San Juan during the day, but by the early evening that difference was 2.44°C (Figure 5), indicating rapid cooling after sunset. The smaller nighttime ΔT_{CBD-HB} values were calculated between the CBD and HOBOs within the urban area of San Isidro. HOBO 2S, for example, is located within the town of San Isidro and it remains within 1°C of the CBD throughout the evening (Figure 6), indicating the presence of a strong UHI at this site.

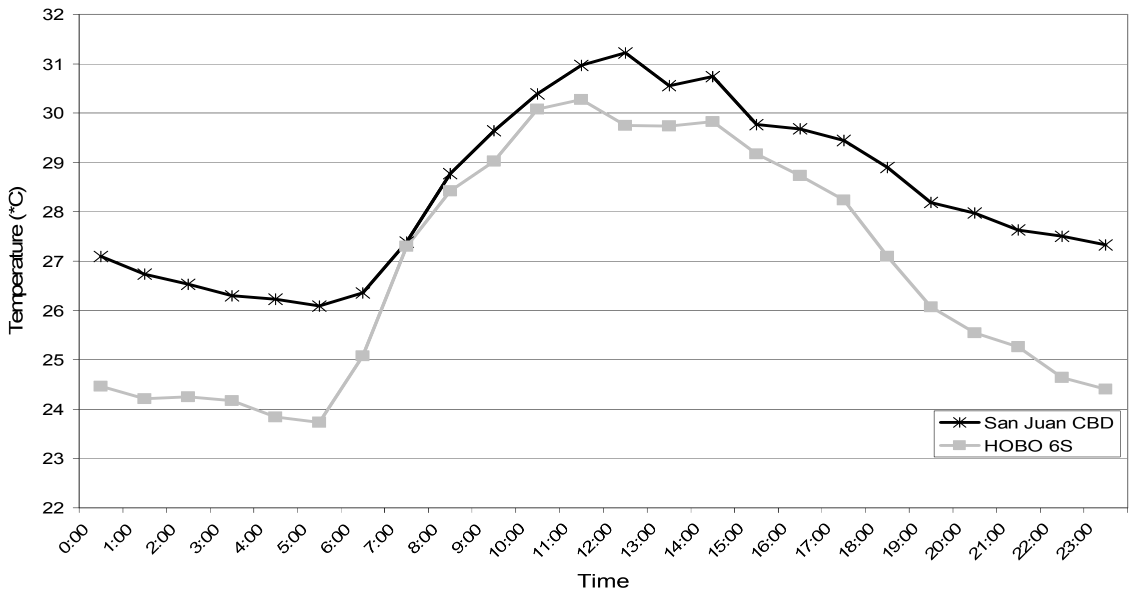

Figure 5. Comparison of the average diel temperature trends between the San Juan central business district (CBD) and HOBO 6S, located in a mowed grass field upwind of a major shopping complex. CBD data was measured during 6/26/06 – 7/5/06, and HOBO 6S was measured during 7/1/06 – 7/5/06.

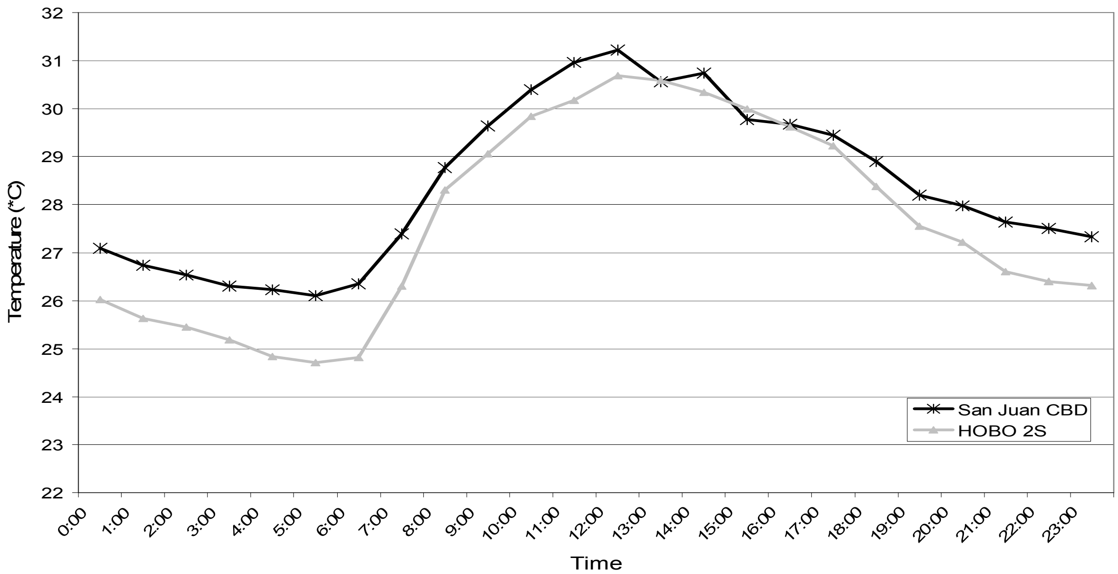

Figure 6. Comparison of the average diel temperature trends between the San Juan central business district (CBD) and HOBO 2S, located within the town of San Isidro, for 6/26/06 – 7/5/06.

The forest site was the only location to register larger $\Delta T_{CBD\text{-}HB}$ values during the day rather than at night. The coolest temperatures of the forest interiors can be seen in Figure 7. The temperature directly outside the forest never matches that of the forest site. A graph of the temperature difference between the forest and outside forest sites indicates rapid warming of the outside the forest site at 0800 hours (Figure 8). The outside the forest site is warmer than the forest site and this persists throughout the night until 0400 hours at which time the temperature decreases rapidly.

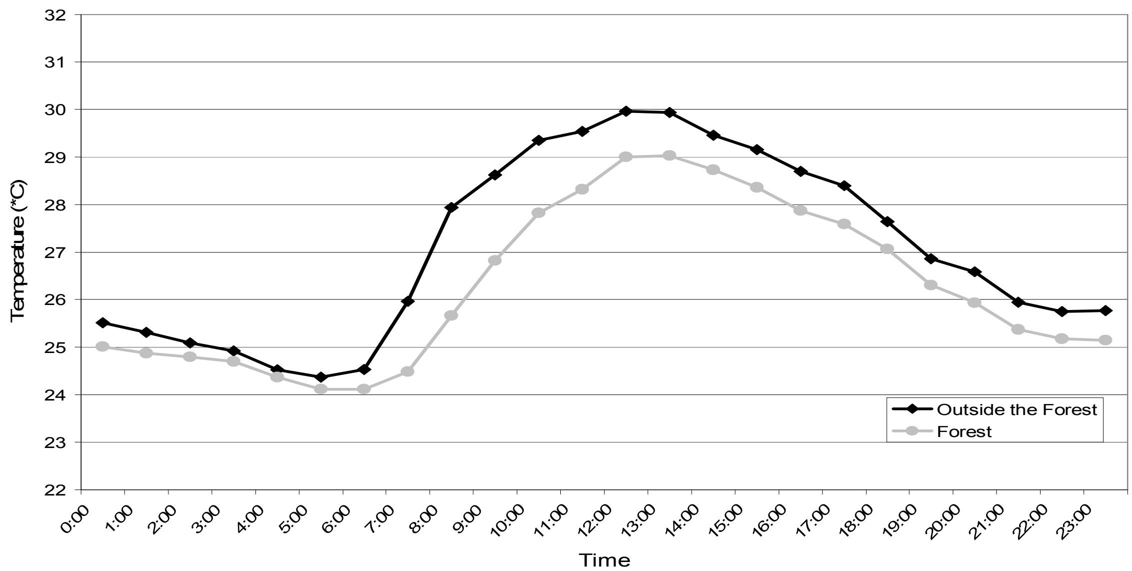

Figure 7. Average diel temperature trends at the forest and outside the forest sites, 6/26/06 – 7/5/06. At no point during the day or night is the temperature of the outside the forest site as high as the forest temperature.

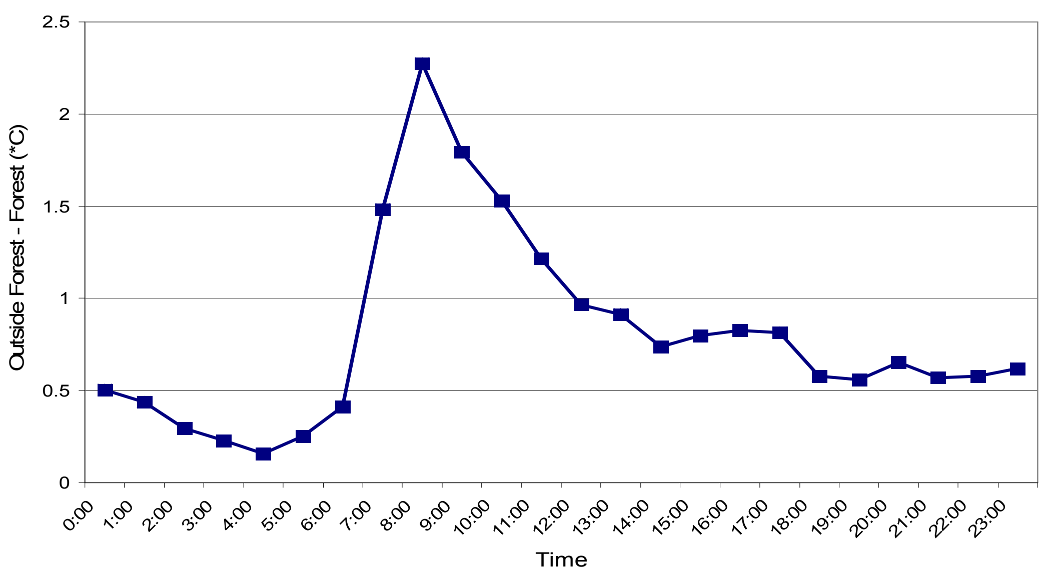

Figure 8. Difference graph, calculated as the temperature difference between the outside the forest site and the forest site, for all hours of the day. The temperature difference is greatest during the early morning.

I compared the CBD, forest, HOBO1S, and HOBO 6S diel temperature data to examine the effects of different land-cover types on air temperature (Figure 9). The CBD was warmer than all other sites throughout the day and night. At the grassland site I found high daytime air temperatures and low nighttime temperatures, while at the forest site temperatures were consistently cooler and at the CBD consistently warmer throughout both the day and night. These trends resulted in large diel temperature ranges at grassland sites, and small diel temperature ranges at both the forest and CBD sites (Figure 10).

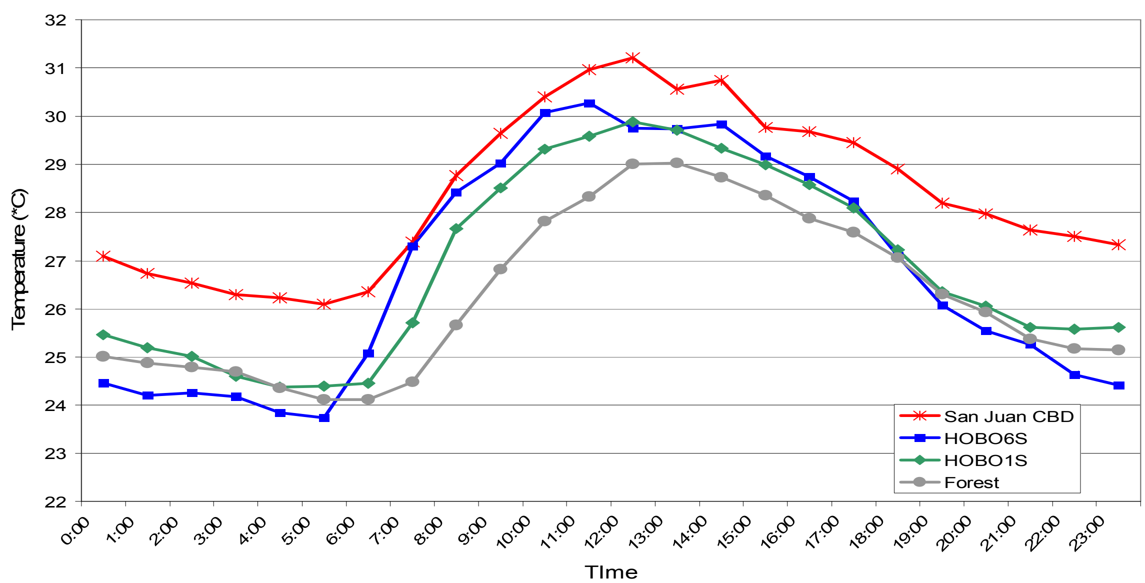

Figure 9. Average diel temperature trends for the central business district (CBD) of San Juan, forest location, HOBO 6S, and HOBO 1S. HOBO 1S is located by an abandoned agricultural field and HOBO 6S is located in a mowed grassland site upwind of a large shopping center at the foothills of the Luquillo Mountains.

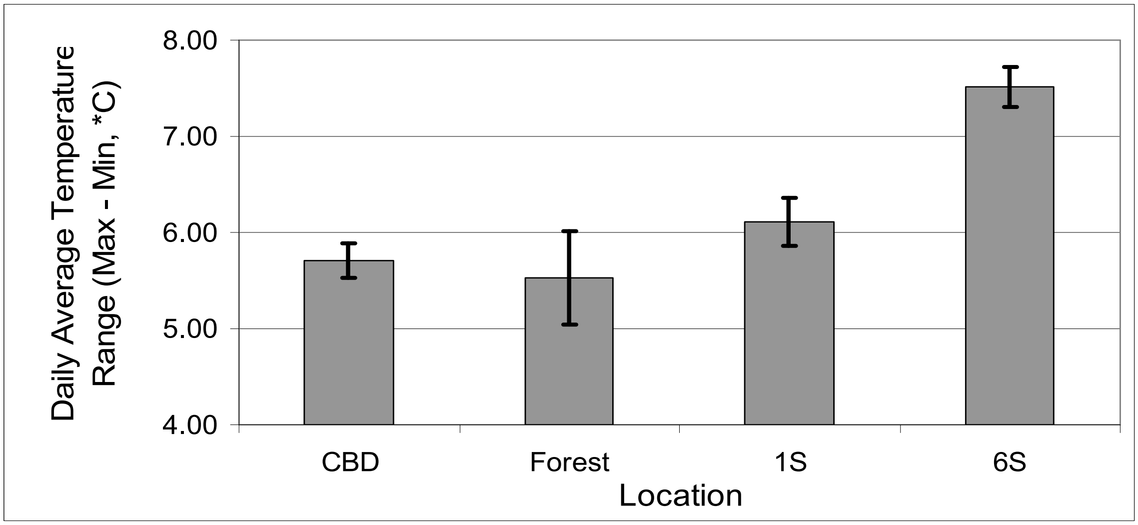

Figure 10. Average diel temperature range, calculated as daily max – daily min, for the central business district (CBD) of San Juan, the forest location, HOBO 1S, and HOBO 6S locations.

2) AIRSHED MODEL RESULTS

Percent vegetation values calculated using east to southeast degree windows and up to around 1300 meters upwind seem to explain variation in temperature collected by the HOBOs the best (Appendix B; Figure 11).

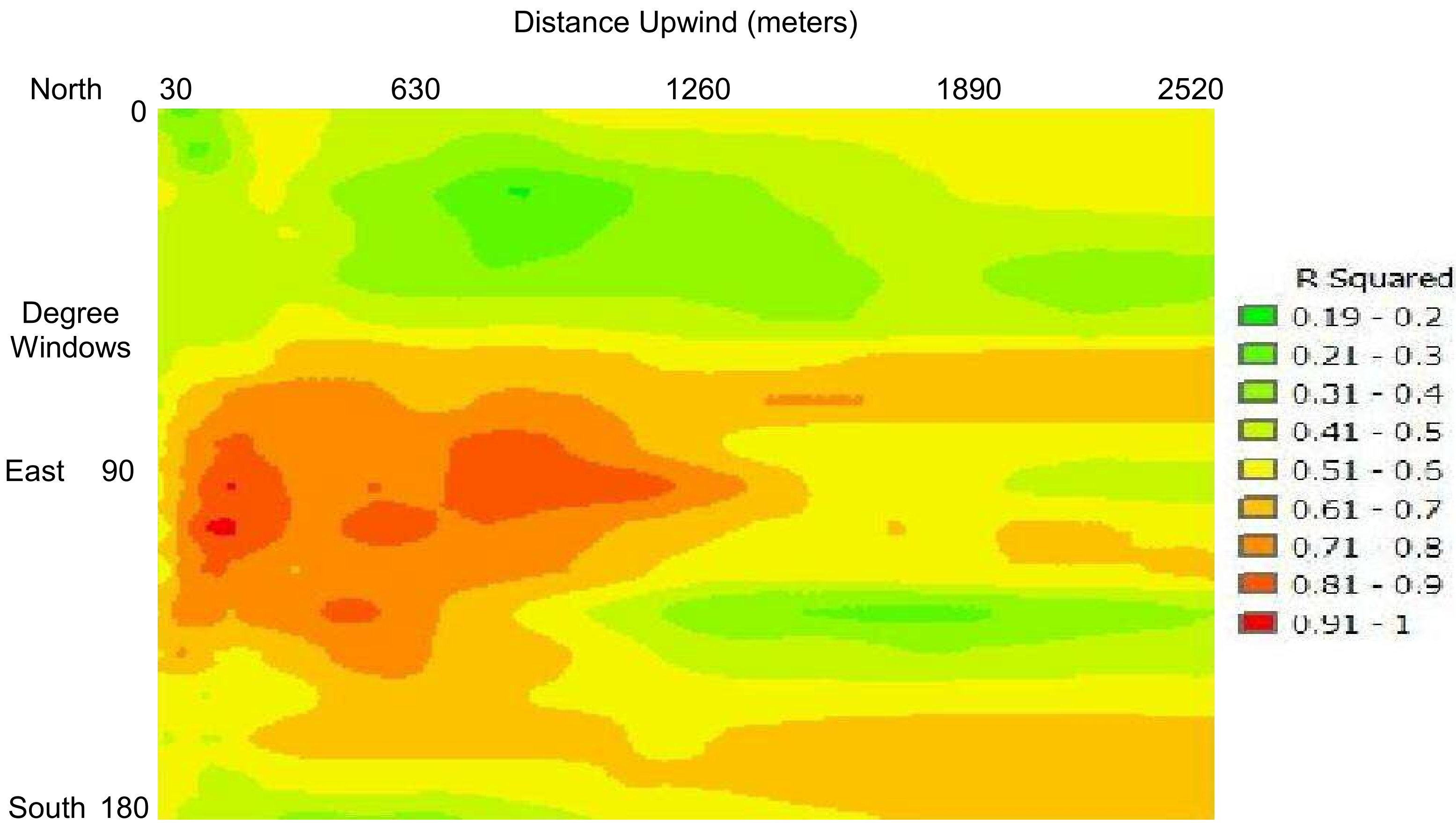

Figure 11. Isocorrelation plot of average temperature data versus percent airshed vegetation along gradient of upwind distance (x) and upwind azimuthal angle (y). Degree windows 10 – 12 (91° - 120°), from 150 to 270 meters upwind, represent the 0.91 – 1.0 isocorrelation, and hence the best airsheds for predicting temperature based on land-cover.

The best-fit regression ($r^2 = 0.94$) obtained was calculated using degree window 11 (angle = 101° - 110°) and an upwind distance of 180 meters (Figure 12; Figure 13). Degree windows 10 – 12 (angle = 91° – 120°), from 150 to 270 meters upwind, all produced r^2 values within the 0.91 – 1.0 isocorrelation, and hence represent the best-fit airshed for predicting temperature based on upwind land-cover. Thus, the high correlation between upwind vegetation and temperature recorded by the HOBOs supports hypothesis (H_4) that there is a relation between temperature and upwind vegetation.

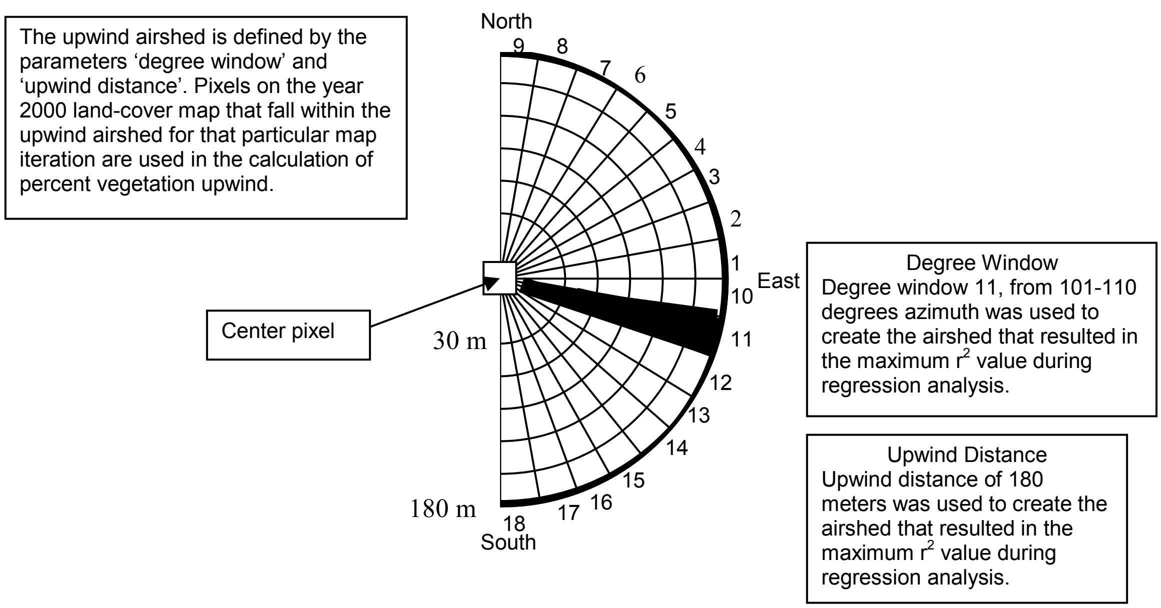

Figure 12. The shaded wedge in the above diagram represents the airshed from which I calculated the percent vegetation value that yielded the maximum r^2 between percent vegetation and average HOBO temperature.

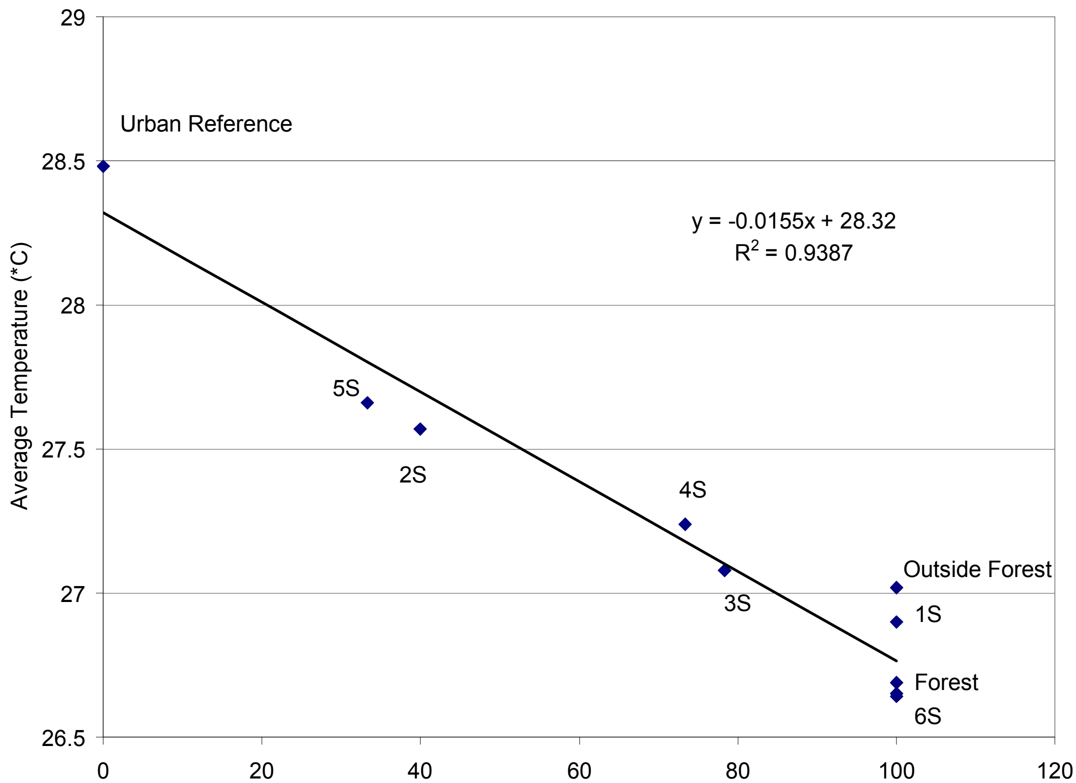

Percent vegetation between 101°and 110° azimuth, and 0 – 180 meters upwind from HOBO locations

Figure 13. Regression analysis of average temperature vs. percent vegetation using degree window 11 and upwind distance 180 meters.

3) AIRSHED MODEL VALIDATION

Comparison of predicted versus observed temperature for the fall HOBO locations (1F – 6F), resulted in an r2 of 0.72 (Figure 14).

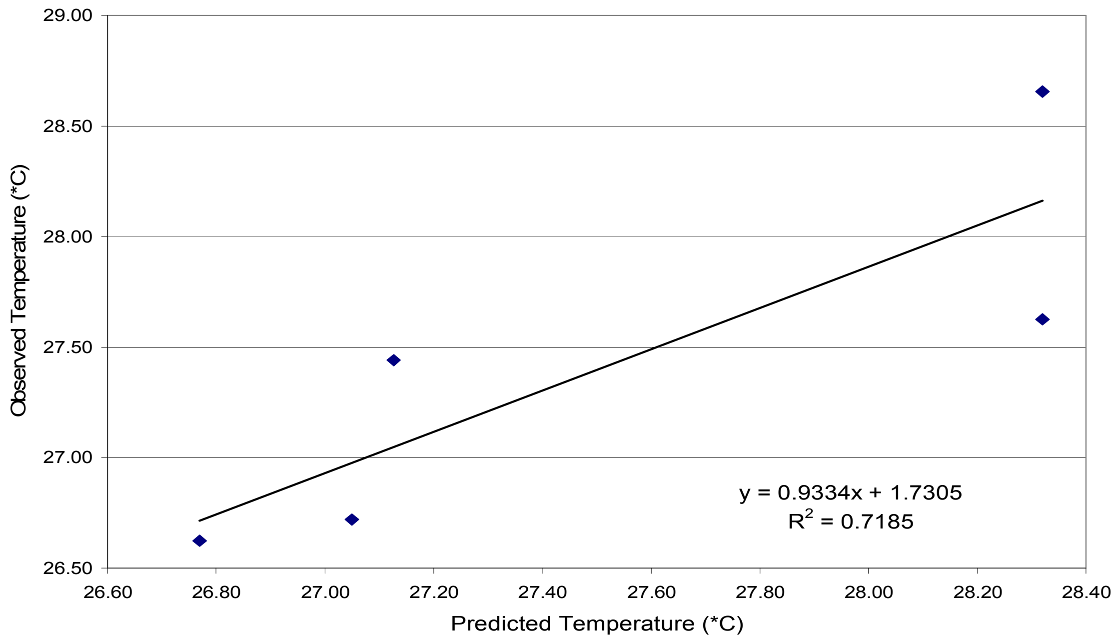

Figure 14. Linear regression between observed and predicted temperature values. The predicted temperature explains the variation in the observed temperature with an r^2 of 0.72

I made average temperature predictions for HOBO 1F-6F using the best-fit regression analysis from the summer data and compared them to the data collected in situ.

Summer Data Regression Equation

Temperature = [-0.0155 * (percent land-cover)] + 28.32

The best-fit regression equation predicted average temperature with a mean absolute error of ±0.36°C (Table 4).

Table 4: Comparison of predicted vs. observed average temperature values for the fall data set. Since some predictions are above and some below the observed values, the absolute value of the temperature difference was used to get the average deviation from observed values. Overall, the summer regression equation predicted temperature well, with mean absolute error of ±0.36°C.

Model Validation

Validation HOBOs	Percent Vegetation	Predicted Temp. (*C)	Observed Temp. (*C)	Mean Error Pre. - Obs.	Mean Absolute Error [Pre - Obs.]
1	0	28.32	28.66	-0.34	0.34
2	0	28.32	27.63	0.69	0.69
3	100	26.77	26.62	0.15	0.15
4	82	27.05	26.72	0.33	0.33
5	77	27.13	27.44	-0.31	0.31
Average		**27.52**	**27.41**	**0.10**	**0.36**

4) URBANIZATION MODEL AND THE FUTURE URBAN HEAT ISALND

Predictive maps of the UHI in northeastern Puerto Rico show intensification of the UHI within the SJMA, and geographic expansion of the UHI, especially towards the Luquillo Mountains (Figure 15a – 15f).

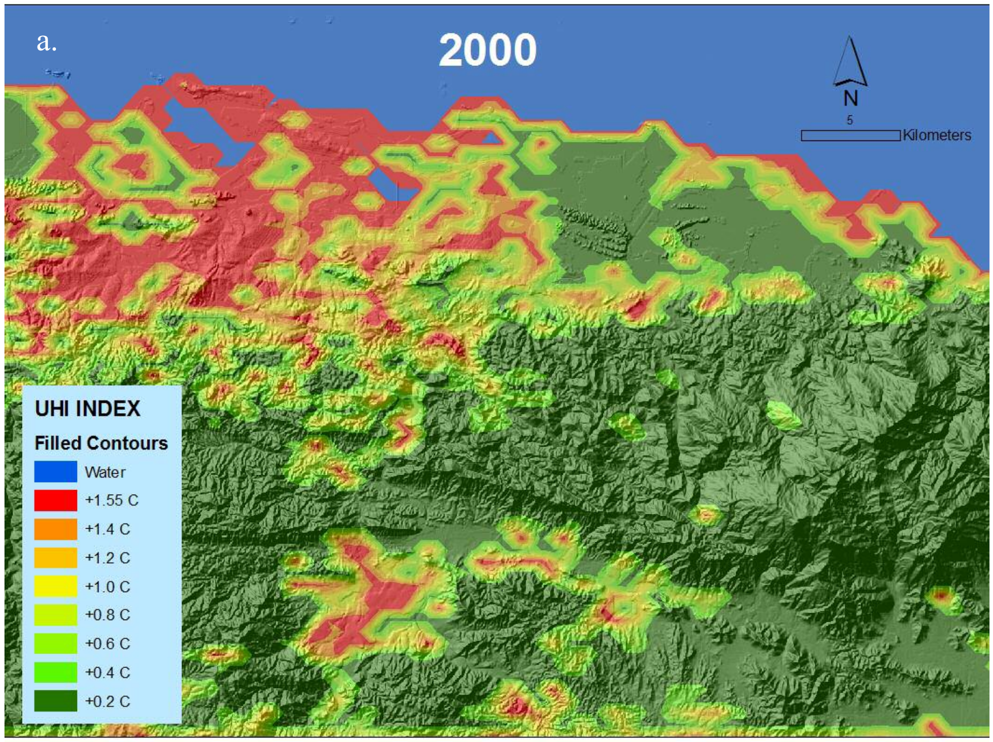
a.
2000
N
5
Kilometers
UHI INDEX
Filled Contours
Water
+1.55 C
+1.4 C
+1.2 C
+1.0 C
+0.8 C
+0.6 C
+0.4 C
+0.2 C

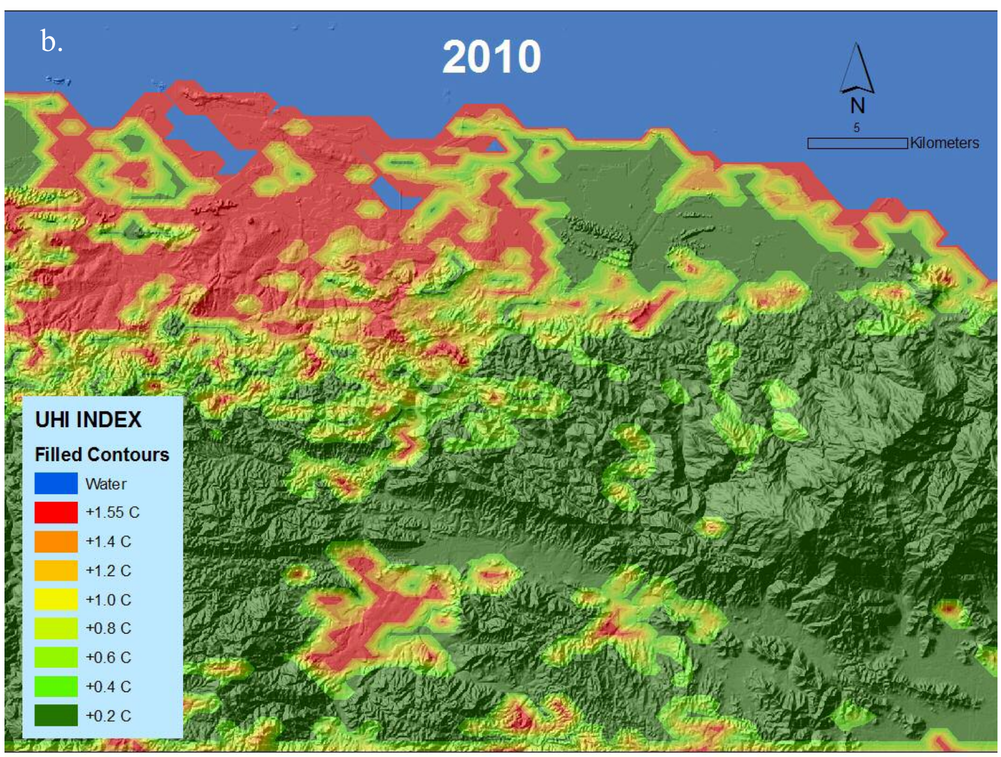
b.
2010
N
5
Kilometers
UHI INDEX
Filled Contours
Water
+1.55 C
+1.4 C
+1.2 C
+1.0 C
+0.8 C
+0.6 C
+0.4 C
+0.2 C

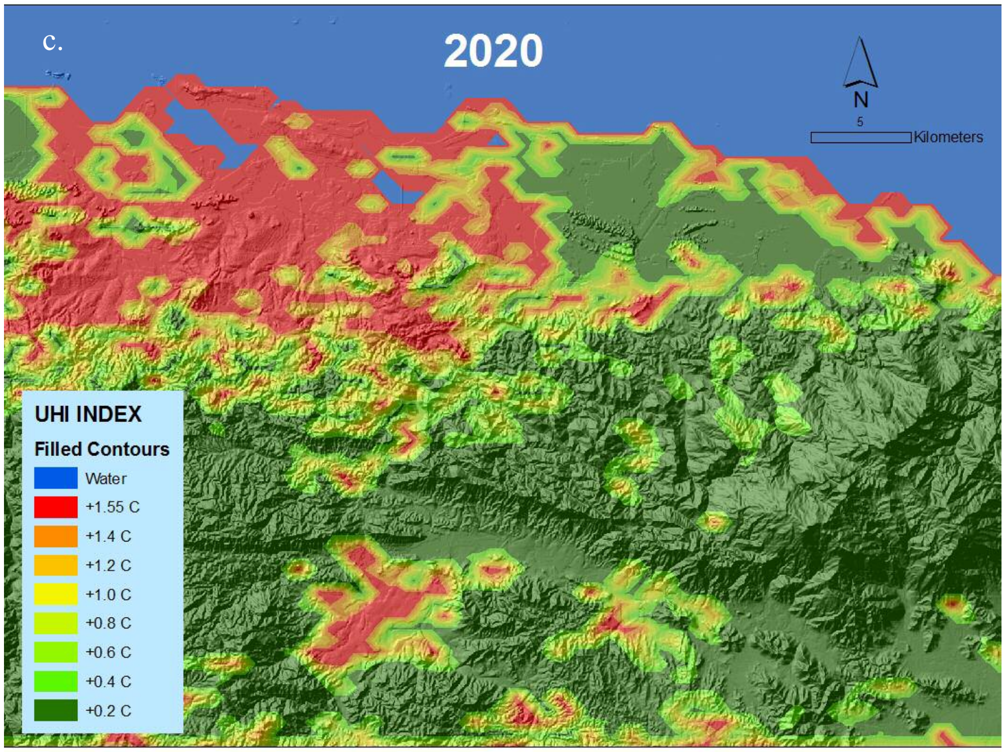
c.
2020
N
5
Kilometers
UHI INDEX
Filled Contours
Water
+1.55 C
+1.4 C
+1.2 C
+1.0 C
+0.8 C
+0.6 C
+0.4 C
+0.2 C

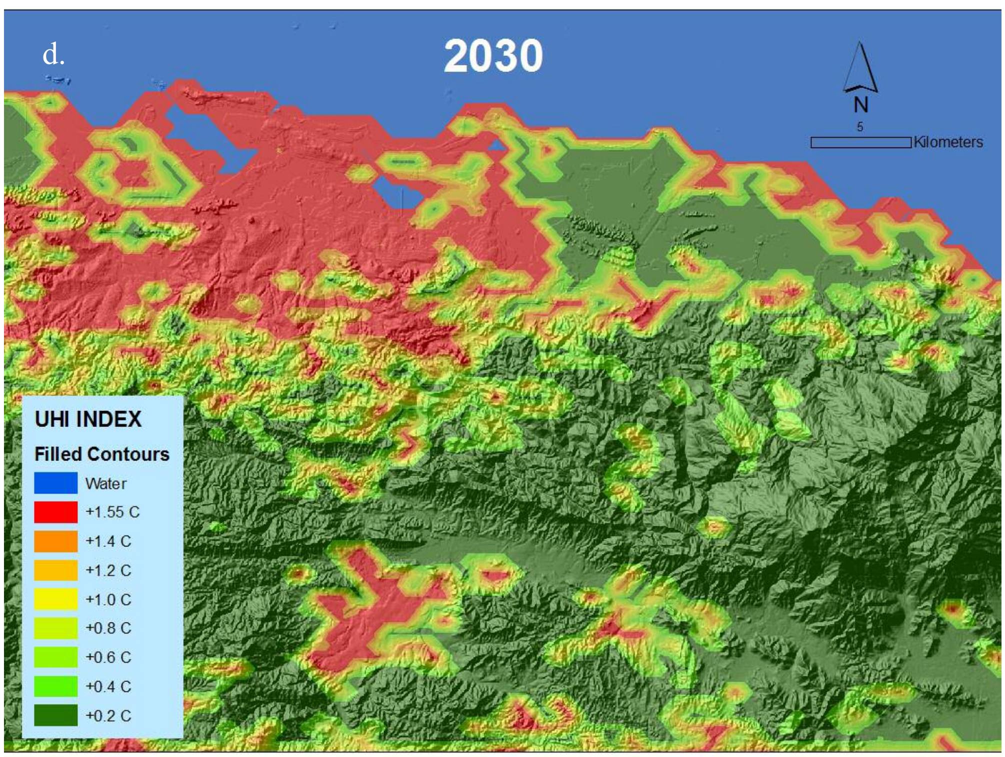
d.
2030
N
5
Kilometers
UHI INDEX
Filled Contours
Water
+1.55 C
+1.4 C
+1.2 C
+1.0 C
+0.8 C
+0.6 C
+0.4 C
+0.2 C

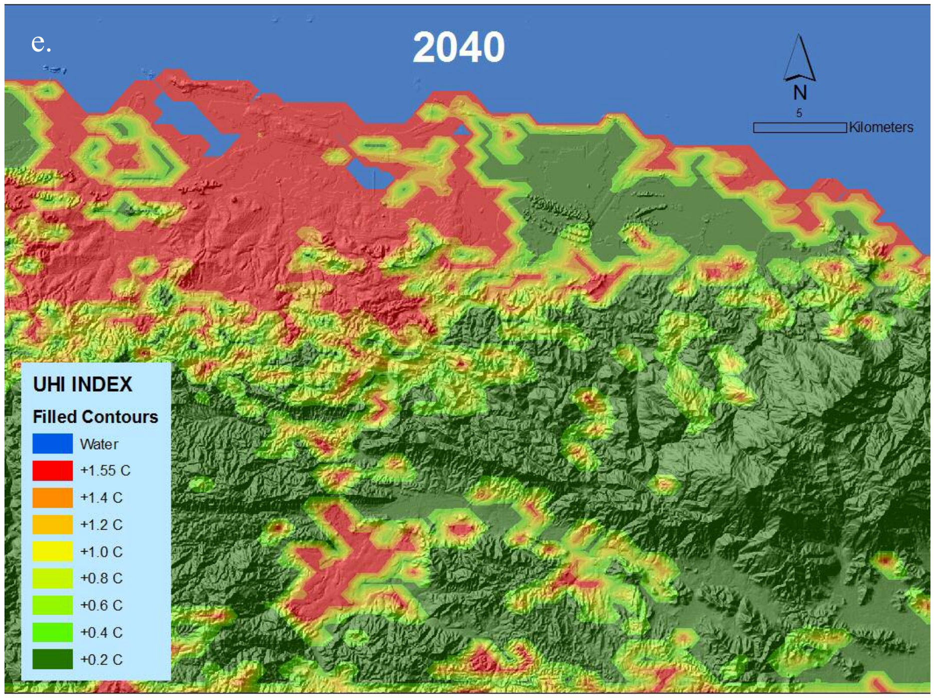

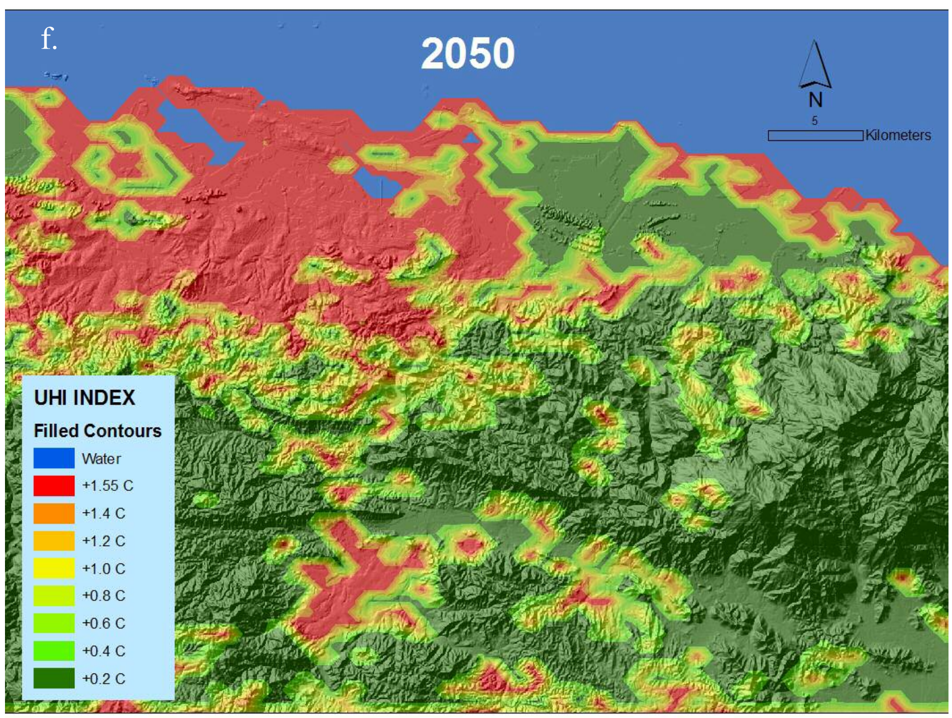

Figure 15: Maps showing the current (a) and projected (b – f) geographic expansion of the UHI in northeastern Puerto Rico.

Between the years of 2000 and 2050, urbanization under the ‘business as usual’ urbanization scenario resulted in declines in the number of pixels with UHI values equal to or less than +0.8°C, while the number of pixels with UHI values greater than +0.8°C increased (Figure 16). More importantly, the greatest changes between years 2000 and 2050 were marked by large decreases of land area with a UHI index equal to or less than +0.2°C, and large increases of land areas with a UHI index of +1.55°C. Over 140 km^2 with a UHI index of +0.2°C was converted to land-cover with a higher UHI index, while over 130 km^2 was converted to a land-cover with a UHI index of +1.55°C (Figure 17).

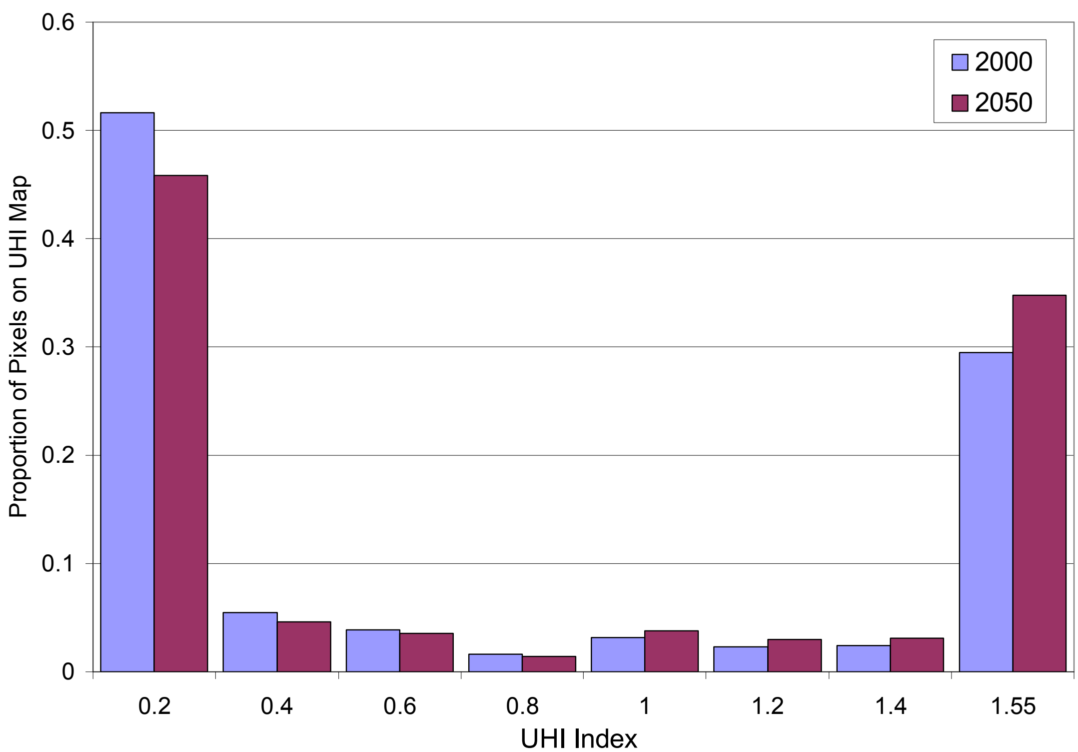

Figure 16. Proportion of pixels on the UHI index maps that fall within each UHI index category for the years 2000 and 2050.

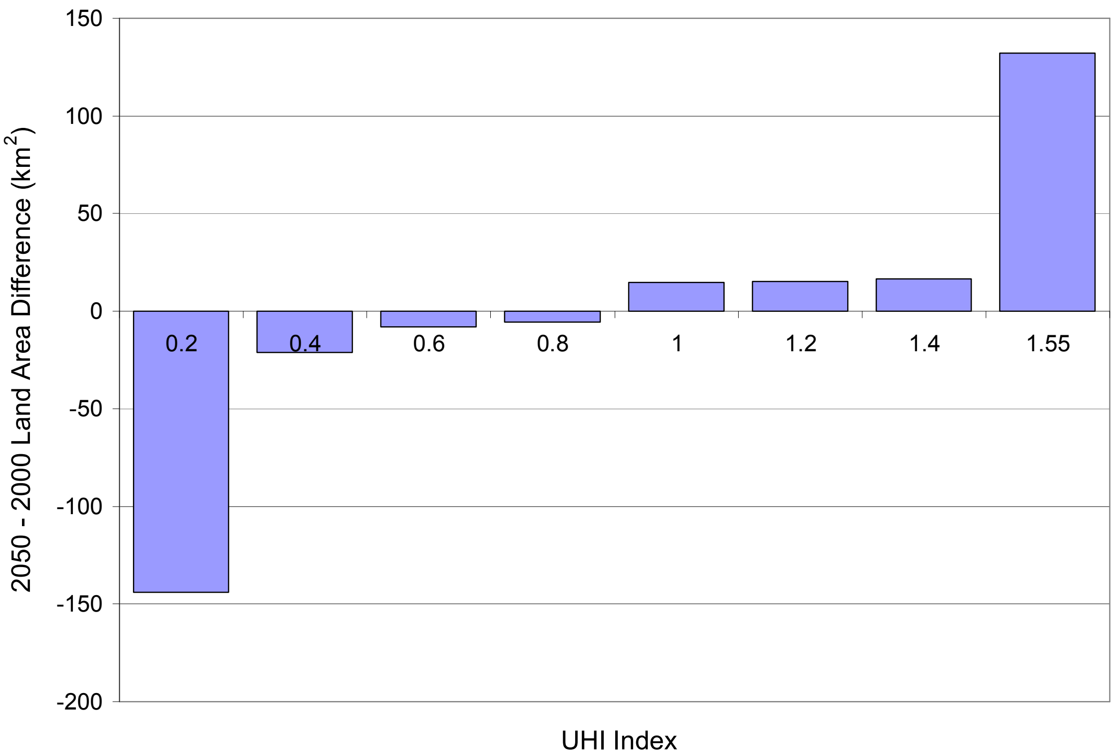

Figure 17. Residual graph representing the land area changes per UHI index category between the years of 2000 and 2050, calculated as number of pixels in 2050 – number of pixels in 2000, per UHI index category.

b. Mobile Measurement Transects

Analysis of temperature (ΔT_{CBD-Tr}) data from the mobile data collection shows considerable variation among r^2 values for different transects calculated as a function of distance from urban center (Figures 18a – 18c), but a clear pattern of cooling with distance from urban center is discernable, thus supporting my hypothesis (2) that the urban heat island effect decreases as the distance from urban center increases. This trend is strongest between 0400 and 0600 hours (Figure 18a) and weakest between 1200 and 1400 hours (Figure 18b), supporting the existence of a late night peak in UHI intensity. I found negligible cooling along the East Route (Rio Grande) between the hours of 2000 and 2200 (Figure 18c), demonstrating that the UHI effect is strong along this route during the early evening. The Rio Grande route ends at the base of the Luquillo Mountains (Figure 2a), supporting hypothesis 3 which states that the UHI is extending to at least the foothills of the Luquillo Mountains. Measurements of $\Delta T_{CBD\text{-}Tr}$ during the hours of 0400 – 0600 and 2000 – 2200 ranged up to more than -2.5°C as distance to urban center increased, while during the hours of 1200 – 1400, $\Delta T_{CBD\text{-}Tr}$ measurements ranged up to only -1°C. These results indicate also the existence of a nocturnal peak in the UHI.

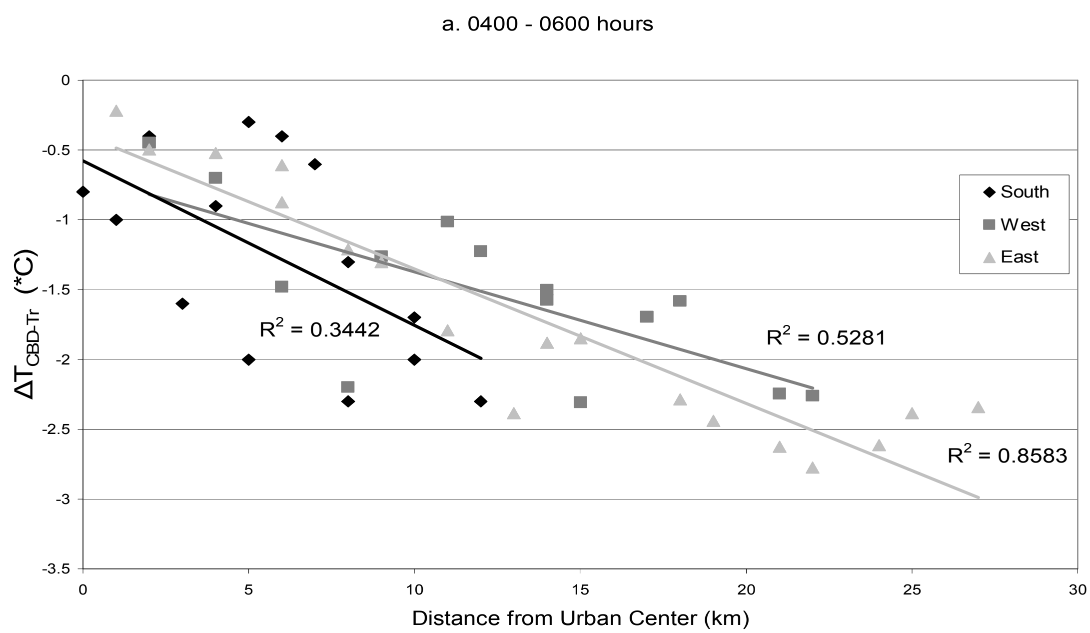

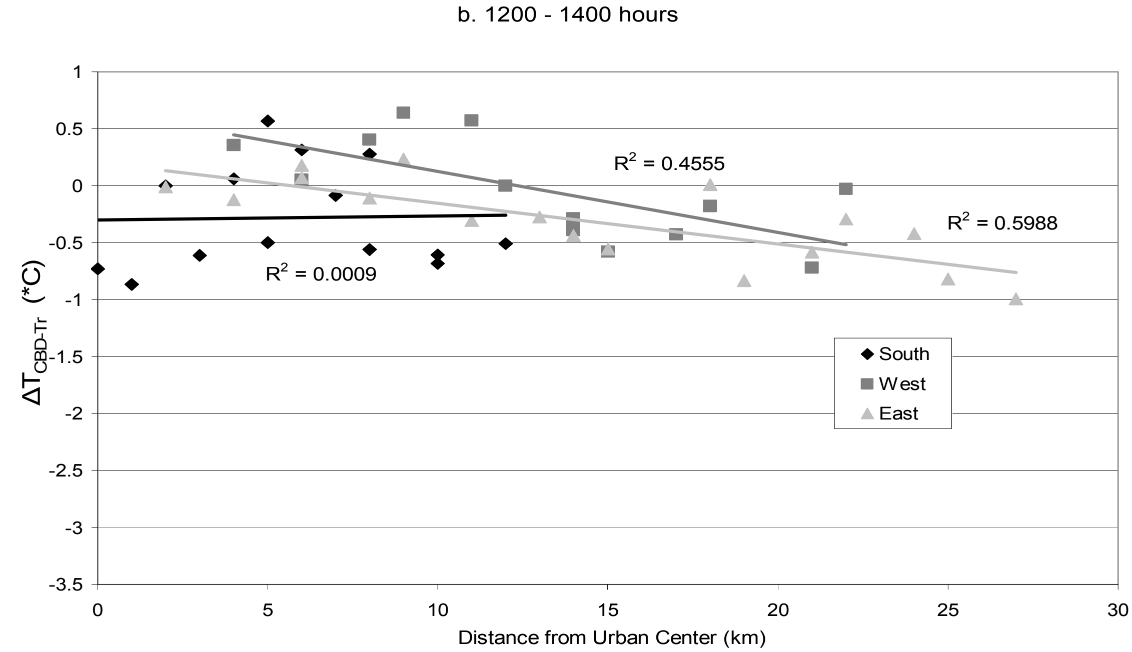

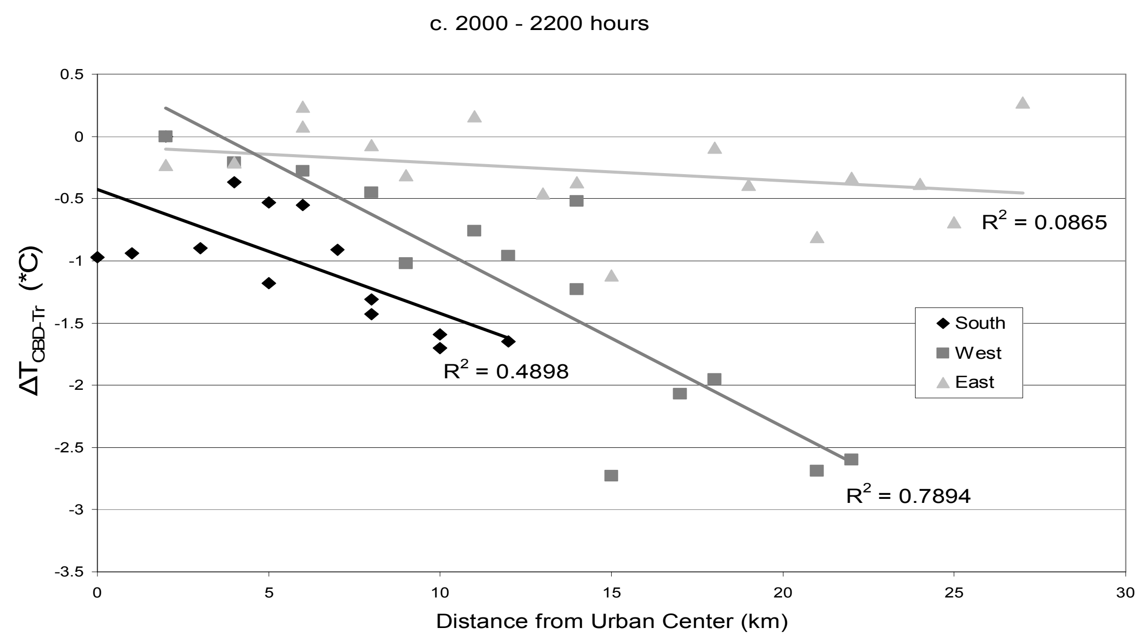

Figure 18. $\Delta T_{CBD\text{-}Tr}$ trends along 3 routes emanating from the San Juan central business district to surrounding rural areas. (a.) Data from all three routes driven between the hours of 0400 – 0600. (b.) Data from all three routes driven between the hours of 1200 – 1400. (c.) Data from all three routes driven between the hours of 2000 – 2200.

6. Discussion

The existence of a pronounced nocturnal UHI is consistent with past UHI studies by Chandler (1965), Oke and East (1971), and Landsberg (1981), and consistent with some but not all findings of Gonzalez et al. (2005). The late morning peak UHI intensity reported by Gonzalez et al. (2005) was recorded by temperature sensors located within the SJMA. It is possible that due to the location of these stations within the SJMA, they may not have captured the urban-rural temperature gradient fully. Instead, these stations may have been reporting diel fluctuations in urban temperature patterns only. Another potential explanation is that the instruments used were positioned too close to impervious surfaces, which reemit longwave radiation throughout the day and night. Gonzalez et al. (2005) reported clear skies during the study which would indicate intense surface warming throughout the day, corroborating this as a possibility.

Rapid warming at the site outside the forest (3A), and at the grassland sites (HOBO 6S and 1S), as opposed to slower warming in the forest site, indicates that tree canopy cover is necessary to mitigate daytime warming. However, the grassland sites cool quickly during the night which indicates that canopy cover is not needed to mitigate the nighttime UHI. Grassland areas allow large amounts of shortwave and longwave radiation to reach the ground and warm the surface during the day, but unlike concrete, grass cannot store large quantities of thermal energy, resulting in quick and pronounced cooling during the evening. This is also demonstrated by the large diel temperature ranges at the grassland sites.

Both the forest and the CBD have small diel temperature ranges. The CBD achieves a small diel temperature range by limiting nighttime cooling. The thermal storage capacity of the CBD allows for prolonged warming throughout the night resulting in a small diel temperature range in the urban areas. On the other hand, the forest site has a small diel temperature range because extensive canopy cover limits the amount of incident radiation reaching the forest floor, and high soil moisture allows for continual evaporative cooling, both of which result in minimal warming in the daytime.

According to these results, the presence of grass-covered ‘green space’ will not impede urban warming during the daytime. This is problematic for businesses and homeowners that operate air conditioning units during daytime hours, and whose properties are normally not surrounded by canopy cover. I believe that open green spaces do not retain enough soil moisture in order to utilize evaporative cooling to the extent needed to counteract daytime UHI formation. Evaporative cooling and shading provided by canopy cover are essential to negate the effects of urban warming. This suggests that “greening” efforts to combat UHIs need to focus on increasing canopy-cover and deepening soils instead of creating simply park-like ‘green spaces’.

The lack of a strong signal of changing temperature with distance from the CBD as one traverses the Rio Grande transect is probably due to the fact that this area is one of the most rapidly urbanizing areas around the SJMA. It is of particular importance because it stretches from the coast to the Luquillo Mountains. I witnessed massive development projects at the base of the Luquillo Mountains already underway during the summer of 2006. These projects are converting lowland forests and grasslands to impervious surfaces, with minimal greenspaces and canopy cover. These land-cover changes are likely to result in intense urban warming, as shown by my urbanization/UHI index projections. Data that I collected from the East (Rio Grande) transect suggests the existence of a pronounced UHI in this area already. Furthermore, Velazquez-Lozada et al. (2006) report that the UHI in San Juan is creating large sensible heat exchanges between upper and lower atmosphere. If this is also the case in Rio Grande, air temperature in the upper atmosphere may increase, altering the elevation at which condensation occurs and hence orographic cloud formation within the Luquillo Mountains.

Development projects such as those in Rio Grande will create UHIs that will impact areas beyond the actual development site. According to the model and regression analyses performed here, areas downwind of these developments will be impacted. Maintenance of tree canopy cover and soil moisture retention should be planned for during these development projects in order to avoid intense daytime warming.

Future modeling efforts should focus attention in two areas. More detailed modeling using land-cover data specific to the type of vegetation present is needed. This will allow researchers to quantify explicitly the effect of percent canopy cover (e.g. grassland = 0%, dense forest = 100%) on UHI formation. Time-series analyses of upwind land-cover using in situ wind direction and velocity data will allow for real-time modeling of the UHI at different locations. A long term product of this research could be a dynamic representation of the UHI created by the SJMA accessible in real-time via internet.

The largest changes in the projected UHI index between 2000 and 2050 occur in the +0.2 °C category, indicating that urbanization is expanding geographically to vegetated areas rather than becoming more intense within previously established urban or suburban areas. Much of this urbanization is concentrated in lands to the southeast, towards the Luquillo Mountains, which is consistent with my observations. My results relating land-cover and the UHI, in addition to the findings of Scatena (1998b), that land-cover change throughout the island is influencing cloud formation and rainfall patterns within the Luquillo Mountains, highlight the need for research that explicitly studies the effect of land-cover change on orographic cloud formation within the Luquillo Mountains. Specifically, future research efforts should focus on the effects of deforestation, suburbanization, and urbanization on the lifting condensation level so as to provide more detailed information pertaining to the future of the freshwater supply for the SJMA.

7. Conclusion

Fixed-station and mobile measurement data show the presence of a nocturnal peak in UHI intensity. The forest site is the only site able to negate urban warming throughout the day. This effect is believed to be because of removal of latent heat via evaporative cooling within the canopy and soil. Grassland sites showed significant daytime warming, but also pronounced nighttime cooling, resulting in large diel temperature ranges. Therefore, human efforts to combat UHI formation need to focus on maintaining canopy cover in order to counteract the UHI effect.

Development projects encroaching on the Luquillo Mountains may impact regional climate by decreasing orographic cloud formation and ultimately water supply to the SJMA. Most of the larger Caribbean Islands have rapid urbanization rates as well, and rely on orographic cloud formation to supply freshwater, so as urbanization continues it will become ever more important to study the effects of UHIs on regional climate in this region.

References

Brazel, A. J., N. Selover, R. Vose, and G. Heisler., 2000: The tale of two climates - Baltimore and Phoenix urban LTER sites. *Climate Research*, **15,** 123-135.

Brown, S., A. E. Lugo, S. Silander, and J. Leigel, 1983: Research history and opportunities in the Luquillo Experimental Forest. Southern Forest Experimental Station, New Orleans, Louisiana. United States Forest Service

Carbone, G., 2004: *Exercises for Weather and Climate*. Fifth ed. Pearson Education, Inc.

Chandler, T. J., 1965: *The Climate of London*. Hutchinson.

Comrie, A. C., 2000: Mapping a wind-modified urban heat island in Tucson, Arizona (with comments on integrating research and undergraduate learning). *Bulletin of the American Meteorological Society*, **81,** 2417-2431.

Daly, C., E. H. Helmer, and M. Quiñones, 2003: Mapping the climate of Puerto Rico, Vieques and Culebra. *International Journal of Climatology*, **23,** 1359-1381.

Dixon, G. P. and T. L. Mote, 2003: Patterns and causes of Atlanta's urban heat island-initiated precipitation. *Journal of Applied Meteorology*, **42,** 1273-1284.

Douglas, I., 1983: The Energy Balance of the City. *The Urban Environment*, Arnold.

Fast, J. D., J. C. Torcolini, and R. Redman, 2005: Pseudovertical temperature profiles and the urban heat island measured by a temperature datalogger network in Phoenix, Arizona. *Journal of Applied Meteorology*, **44,** 3-13.

Gonzalez, J., Jeffery C. Luvall, Douglas Rickman, Daniel Corazamy, Ana Picon, Eric Harmsen, Hamed Parsiani, Ramon E. Vasquez, Nezario Ramirez, Robin Williams, Robert W. Waide, and Craig A. Tepley, 2005: Urban heat islands developing in coastal tropical cities. *EOS, Transactions, American Geophysical Union*, **86,** 397.

Hawkins, T. W., A. J. Brazel, W. L. Stefanov, W. Bigler, and E. M. Saffell, 2004: The role of rural variability in urban heat island determination for Phoenix, Arizona. *Journal of Applied Meteorology*, **43,** 476-486.

Hedquist, B. C. and A. J. Brazel, 2006: Urban, residential, and rural climate comparisons from mobile transects and fixed stations: Phoenix, Arizona. *Journal of the Arizona-Nevada Academy of Science*, **38,** 77-87.

Heisler, G., J. Walton, S. Grimmond, R. Pouyat, K. Belt, D. Nowak, I. Yesilonis, and J. Hom, 2006: Land-cover influences on air temperature in and near Baltimore, MD. *International Conference on Urban Environment*, Gotheburg, Sweden.

Helmer, E. H. and B. Ruefenacht, 2005: Cloud-free satellite image mosaics with regression trees and histogram matching. *Photogrammetric Engineering and Remote Sensing*, **71,** 1079–1089.

Hulme, M. and D. Viner, 1995: A climate change scenario for assessing the impact of climate change on tropical rain forests. A report for the World Wildlife Service by the Climatic Research Unit, School of Environmental Sciences, University of East Anglia, Norwich, UK.

IDRISI Kilimanjaro. 1973: Clark Labs

Jansson, A., C. Folke, J. Rockstrom, and L. Gordon, 1999: Linking freshwater flows and ecosystem services appropriated by people: the case of the Baltic Sea drainage basin. *Ecosystems*, **2,** 351-366.

Landsberg, H. E., 1981: *The Urban Climate*. Vol. 28, *International Geophysics Series*, Academic Press.

Larsen, M. C., 2000: Analysis of 20th century rainfall and streamflow to characterize drought and water resources in Puerto Rico. *Physical Geography*, **21,** 494-521.

McDonnell, M. J. and S. T. A. Pickett, 1990: Ecosystem structure and function along urban-rural gradients: an unexploited opportunity for ecology. *Ecology*, **71,** 1232-1237.

Millan, M. M., M. J. Estrela, and M. J. Sanz, 2005: Climatic feedbacks and desertification: The Mediterranean Model. *Journal of Climate*, **18,** 684-701.

Morris, C. J. G., I. Simmonds, and N. Plummer, 2001: Quantification of the influences of wind and cloud on the nocturnal urban heat island of a large city. *Journal of Applied Meteorology*, **40,** 169-182.

Odum, H. T., G. Drewry, and J. R. Kline, 1970: Climate at El Verde, 1963 - 1966. *A Tropical Rain Forest: a study of irradiation and ecology at El Verde, Puerto Rico*, H. T. Odum, Ed., Division of Technical Information, U.S. Atomic Energy Commission.

Oke, T. R. and C. East, 1971: The urban boundary layer in Montreal. *Boundary Layer Meteorology*, **1,** 411-437.

Oke, T. R., 1973: City size and the urban heat island. *Atmospheric Environment*, **7,** 769-779.

Oke, T. R., 1976: The distinction between canopy and boundary layer urban heat islands. *Atmosphere*, **14,** 268-277.

Onset Computer Corporation. PO Box 3450, Pocasset, MA 02559-3450

Panofsky, H. A. and J. A. Dutton, 1984: *Atomspheric Turbulence*. John Wiley, 397 pp.

Pontius Jr., R. G., J. D. Cornell, and C. A. S. Hall, 2001: Modeling the spatial pattern of land-use change with GEOMOD2: application and validation for Costa Rica. *Agriculture, Ecosystems, and Environment*, **85,** 191 - 203.

Rosenfeld, D., 2000: Suppression of rain and snow by urban and industrial air pollution. *Science*, **287,** 1793-1796.

Scatena, F. N., 1998a: Climate change and the Luquillo Experimental Forest of Puerto Rico: assessing the impacts of various climate change scenarios. *American Water Resources Association TPS*, **98,** 91-96.

Scatena, F. N., 1998b: An assessment of climate change in the Luquillo Mountains of Puerto Rico. *Third International Symposium on Water Resources, Fifth Caribbean Islands Water Resources Congress, American Water Resources Association*, 193 - 198.

Stull, R. B., 2000: *Meteorology: for scientists and engineers*. Second ed. Brooks/Cole.

Summers, P. W., 1964: An urban ventilation model applied to Montreal, Ph.D. Dissertation, McGill University.

UN-POP, 2004: World Population Prospects: The 2004 Revision. Population Division of the Department of Economic and Social Affairs of the United Nations Secretariat. http://esa.un.org/unpp

van der Molen, M. K., 2002: *Meteorological Impacts of Land Use Change in the Maritime Tropics*. Academisch Proefschrift.

Velazquez-Lozada, A., J. Gonzalez, and A. Winter, 2006: Urban heat island effect analysis for San Juan, Puerto Rico. *Atmospheric Environment*, **40,** 1731-1741.

World Resources Institute. 2006. www.earthtrends.org

Wu, W., C. Hall, and L. Zhang, 2006: Predicting the temporal and spatial probability of orographic cloud cover in the Luquillo Experimental Forest in Puerto Rico using generalized linear (mixed) models. *Ecological Modeling*, **192,** 473-498.

Appendix A

Fortran Code for Airshed Model
(Comments within the code are in *italics*)

```
PROGRAM airshed
implicit none

!OBJECTIVES**************************************************************
!I calculated percent vegetation in the upwind direction by creating an
!airshed whose dimensions were determined by azimuth degree and upwind
!distance parameters. There are a total of 180 azimuth degrees,
!from due north to due south, and a maximum of 2520 meters upwind.
!I divided the azimuth degrees into 18 windows of 10 degrees each,
!termed "degree window", and since the year 2000 land-cover map has a
!resolution of 30 meters, I iterated the "upwind distance" variable
!using 30 meter increments. The model begins on a 'center pixel' by
!selecting the first of the 18 degree windows and the first of the
!upwind distances from which it forms the airshed. The percent
!vegetation is calculated for the airshed, and the resulting
!percentage is assigned to the center pixel. This process is repeated
!for every pixel on the map using the first degree window and the
!first upwind distance. Then the model changes to the second
!upwind distance value and the calculation is repeated for the entire
!map. Once the model iterates through all upwind distances using
!"degree window 1", it will switch to "degree window 2" and the entire
!process is repeated. With 18 degree windows and 84 upwind distances
!(2520 maximum upwind distance/30 meter increments), the model performs
!a total of 1512 iterations of the entire map.
!************************************************************************
```

```
!DICTIONARY************************************************************
!row = integer dimensioning rows on the map
!col = integer dimensioning columns on the map
!vector = integer used to iterate the vector do-loop
!numvecs = integer value used to dimension the maximum extent of the vector do-loop
!sd = the degree value to begin the degree do-loop with
!ed = the degree value to end the degree do-loop with
!vec = integer used to identify the number of upwind distances to be used in the model
!nrow   = integer stating the number of rows in the map
!ncol   = integer stating the number of columns in the map
!vectorY = integer value used to parameterize the airshed in the y direction upwind
!vectorX = integer value used to parameterize the airshed in the x direction upwind
!degree = the degrees used to create the 'degree window', expressed in degrees
!quad1 = integer to iterate the degree windows in quad 1 of a Cartesian Plane,
!       or from due east to due north using cardinal directions
!quad4 = integer to iterate the degree windows in quad 4 of a Cartesian Plane,
!        or from due east TO due south using cardinal directions
!counter = integer used to iterate the degree windows
!vectorh = hypotenuse of the fetch window, squared
!waterpix = variable used to count the number of water pixels within the airshed
!nonvegpix = variable used to count the number of non-vegetation pixels within the airshed
!vegpix  = variable used to count the number of vegetation pixels within the airshed
!angle = the direction of the wind represented in radians
!drconv = conversion constant from degrees to radians
!landcover = variable used to dimension the landcover map used by the program
!vegcover = variable used to the calculate the percent vegetation cover within each airshed
!**********************************************************************

!NOTE******************************************************************
!When describing wind direction as North, we usually use 0/360 degrees.
```

```
!Fortran uses a mathematical cartesian plane, therefore due north is
!actually at 90 degrees. For example, in order to represent the easterly winds in
!PR, which are normally around 80 degrees on weather charts, I must
!use 10 degrees in Fortran. Then convert that into radians.
!*********************************************************************



!DECLARATION OF VARIABLES**********************************************
INTEGER                                 :: row, col, vector, numvecs, Fdist, sd, ed, vec
INTEGER, PARAMETER                      :: nrow = 706, ncol = 1621
INTEGER                                 :: vectorY, vectorX, degree, quad1, quad4, counter, vectorh
REAL                                    :: waterpix, nonvegpix, vegpix, angle, drconv
INTEGER, ALLOCATABLE, DIMENSION(:,:)    :: landcover
REAL, ALLOCATABLE, DIMENSION(:,:)       :: vegcover
!*********************************************************************

!OPEN FILES************************************************************
open (1,FILE="C:\DaveM\PR_summer_06\Modeling\numvecs3\lu_00_reclass_smallw_asc.rst", status = "unknown")
open (2,FILE="C:\DaveM\PR_summer_06\Modeling\numvecs3\fetch_quad1+4_metadata.txt", status = "unknown")
open (3,FILE="C:\DaveM\PR_summer_06\Modeling\numvecs3\fetch_quad1_output.txt", status = "unknown")
open (4,FILE="C:\DaveM\PR_summer_06\Modeling\numvecs3\fetch_quad4_output.txt", status = "unknown")
!*********************************************************************

!ALLOCATION OF VARIABLES***********************************************
ALLOCATE (landcover(nrow,ncol))
ALLOCATE (vegcover(nrow,ncol))
!*********************************************************************

DO row = 1, nrow
  DO col = 1, ncol
```

```
    READ (1,*) landcover(row,col)
    !write (*,*) landcover(row,col)
  END DO
END DO
!**********************************************************************
counter = 0
quad1 = 0
quad4 = 0
drconv = 0.0174532925
vec = 0

!Two large do-loops are used to represent quad 1 and quad 4 on a cartesian plane,
!or from east to north and from east to south.

DO quad1 = 1,9

!the counter is used to iterate the degree windows.

  counter = counter + 1
  DO vec = 1, 84

!84 vectors equals max upwind distance divided by map resolution (2520/30).
!Numvecs is used to adjust the vectors in the later do-loops. If vec = 12, for instance,
!and the maximum upwind distance used in the model is still 2520 meters, then
!each upwind distance iteration must cover 210 meters, rather than 30 meters (210*12 = 2520)
!Therefore each vector loop must cover 210 meters rather than 30 meters. In this example,
!numvecs would equal 6, because 6*30 meter resolution = 210.

  numvecs = 1*vec
```

```
!counter is used to iterate the degree window
    select case (counter)
      case (1)
        sd = 1
        ed = 10
      case (2)
        sd = 11
        ed = 20
      case (3)
        sd = 21
        ed = 30
      case (4)
        sd = 31
        ed = 40
      case (5)
        sd = 41
        ed = 50
      case (6)
        sd = 51
        ed = 60
      case (7)
        sd = 61
        ed = 70
      case (8)
        sd = 71
        ed = 80
      case (9)
        sd = 81
        ed = 90
      case default
    end select
```

!Because this is a fetch model, I needed to make sure that the map had ample pixels
!in the upwind direction to make all the calculations. To do this I constructed a border around
!the map by indenting the row and column variables. Due to the large size
!of the map, this did not impact the calculation of upwind vegetation for my
!locations of interest.

```
   DO row = 95, nrow - (numvecs+2)
     DO col = 1, ncol - (numvecs+2)
       vegpix = 0
       waterpix = 0
       nonvegpix = 0

         DO degree = sd,ed
           angle = degree*drconv
           !WRITE (*,*) angle

             DO vector = 1, numvecs
```

!The following lines calculate the vectors for both the x and y directions forming the airshed.
!Row values on the map increase from top to bottom, so I must use "row - (trig function)" to get the airshed
!to expand from due east to due north. In the quad 4 do-loop, this same function is "row +(trig function)"
!because the airshed is to expand from due east to due south.

```
               VectorX = NINT (col + (VECTOR * COS(ANGLE)))
               VectorY = NINT (row - (VECTOR * SIN(ANGLE)))
```

!Notice that the dimensioning of landcover below uses vectorY representing row, and vectorX representing column
!This allows vectorX to grow the airshed in the "east-west" direction, which actually changes the column numbers on the
!map, not the row numbers. Vice versa is true for vectorY.

```
                    select case (landcover(vectory,vectorx))

!These numbers correspond to a year 2000 land-cover map of Puerto Rico
!(Helmer, E. H. and B. Ruefenacht, 2005: Cloud-free satellite image mosaics with regression trees and histogram matching.
!Photogrammetric Engineering and Remote Sensing, 71, 1079–1089.)

                     case (10)
                       waterpix = waterpix + 1
                     case (20,30,40,50)
                       vegpix = vegpix + 1
                     case (60,70,80,90)
                       nonvegpix = nonvegpix + 1
                     case default
                    end select
              end do
              ! write (*,*) VECTORx, vectory
            end do

!The following is the calculation of percent vegetation for the airshed for this map iteration
            vegcover(row,col)  = (vegpix/(waterpix + vegpix + nonvegpix))*100
            !write (*,*) vegcover(row,col)
          END do
        End do
!vector h = the square of the hypotenuse distance of the airshed formed by vectoryX in the
!east-west direction, and vectorY in the north-south direction.

      vectorH = vectorx**2 + vectory**2

!this is a metadata file used to record the following information: quad, degree window used to form the airshed,
!hypotenuse distance squared, and number of vectors used to form the upwind distance variable of the airshed
```

```
WRITE (2,*) "quad                              =", "1"
WRITE (2,*) "degree window                     =", quad1
WRITE (2,*) "sqare of vector distance (m^2)   =", vectorh
WRITE (2,*) "number of vectors                 =", numvecs
```

!In order to save time and make data analysis easier, I only output the cells that correspond to HOBO measurements
!recorded in situ during the summer and fall of 2006. The following is a list of all cells corresponding to HOBOs
!1S-6S, R1-R4, and 1F-6F (although not in that order). The cell numbers (row,col) were attained by georeferencing
!the lat/long coordinates for each of the HOBOs in IDRISI and assigning each HOBO to one cell on the map.

```
DO row = 1, nrow
  DO col = 1, ncol
    !write (5,*) vegcover(row,col)

    if (row.EQ.378.and.col.EQ.1132) then
      write (3,*) "1",",", row, ",", col,",", ed, ",", fdist,",", vegcover(row,col)
    end if
    if (row.EQ.377.and.col.EQ.1132) then
      write (3,*) "2",",", row, ",", col,",", ed, ",", fdist,",", vegcover(row,col)
    end if
   if (row.EQ.381.and.col.EQ.1110) then
      write (3,*) "3", ",",row, ",", col,",", ed, ",", fdist,",", vegcover(row,col)
    end if
   if (row.EQ.388.and.col.EQ.1212) then
      write (3,*) "4", ",", row, ",", col,",", ed, ",", fdist,",", vegcover(row,col)
    end if
   if (row.EQ.293.and.col.EQ.1094) then
      write (3,*) "5", ",", row, ",", col,",", ed, ",", fdist,",", vegcover(row,col)
    end if
   if (row.EQ.348.and.col.EQ.1105) then
      write (3,*) "6", ",", row, ",", col,",", ed, ",", fdist,",", vegcover(row,col)
```

```
 end if
 if (row.EQ.404.and.col.EQ.1115) then
    write (3,*) "7", ",", row, ",", col,",", ed, ",", fdist,",", vegcover(row,col)
 end if
 if (row.EQ.385.and.col.EQ.1162) then
    write (3,*) "8", ",", row, ",", col,",", ed, ",", fdist,",", vegcover(row,col)
 end if
 if (row.EQ.252.and.col.EQ.511) then
    write (3,*) "9", ",", row, ",", col,",", ed, ",", fdist,",", vegcover(row,col)
 end if
if (row.EQ.428.and.col.EQ.1126) then
    write (3,*) "10", ",", row, ",", col,",", ed, ",", fdist,",", vegcover(row,col)
end if
if (row.EQ.398.and.col.EQ.1285) then
    write (3,*) "11", ",", row, ",", col,",", ed, ",", fdist,",", vegcover(row,col)
end if
if (row.EQ.395.and.col.EQ.1299) then
    write (3,*) "12", ",", row, ",", col,",", ed, ",", fdist,",", vegcover(row,col)
end if
if (row.EQ.406.and.col.EQ.1299) then
    write (3,*) "13", ",", row, ",", col,",", ed, ",", fdist,",", vegcover(row,col)
end if
if (row.EQ.421.and.col.EQ.1323) then
    write (3,*) "14", ",", row, ",", col,",", ed, ",", fdist,",", vegcover(row,col)
end if
if (row.EQ.427.and.col.EQ.1336) then
    write (3,*) "15", ",", row, ",", col,",", ed, ",", fdist,",", vegcover(row,col)
end if
if (row.EQ.436.and.col.EQ.1321) then
    write (3,*) "16", ",", row, ",", col,",", ed, ",", fdist,",", vegcover(row,col)
END if
```

```
         END DO
      END DO
  END DO
END DO

!*************************************************************************

!The following is an exact replica of the above code, except for the aforementioned difference in
!the calculation of the airshed using the trig. functions. Therefore most comments have been omitted.

counter = 0
quad1 = 0
quad4 = 0
drconv = 0.0174532925
vec = 0
DO quad4 = 1,9
   counter = counter + 1
  DO vec = 1,84
   numvecs = 1*vec
      select case (counter)
         case (1)
            sd = 1
            ed = 10
         case (2)
            sd = 11
            ed = 20
         case (3)
            sd = 21
            ed = 30
         case (4)
```

```
      sd = 31
      ed = 40
   case (5)
      sd = 41
      ed = 50
   case (6)
      sd = 51
      ed = 60
   case (7)
      sd = 61
      ed = 70
   case (8)
      sd = 71
      ed = 80
   case (9)
      sd = 81
      ed = 90
   case default
end select

      DO row = 95, nrow - (numvecs+2)
         DO col = 1, ncol - (numvecs+2)
            vegpix = 0
            waterpix = 0
            nonvegpix = 0

            DO degree = sd,ed
               angle = degree*drconv
               !WRITE (*,*) angle
               DO vector = 1, numvecs
```

!Rows on the map increase from top to bottom, so I must use "row + (trig function)" to get the airshed to grow
!from due east to due south

```
                  VectorX = NINT (col + (VECTOR * COS(ANGLE)))
                  VectorY = NINT (row + (VECTOR * SIN(ANGLE)))
                    select case (landcover(vectory,vectorx))
                      case (10)
                        waterpix = waterpix + 1
                      case (20,30,40,50)
                        vegpix = vegpix + 1
                      CASE (60,70,80,90)
                        nonvegpix = nonvegpix + 1
                      case default
                    end select
              END do
              ! write (*,*) VECTORx, vectory
            END DO
            vegcover(row,col)  = (vegpix/(waterpix + vegpix + nonvegpix))*100
            !write (*,*) vegcover(row,col)
          END do
        End do

      vectorH = vectorx**2 + vectory**2
     WRITE (2,*) "quad                          =", "4"
     WRITE (2,*) "map number                    =", quad4
     WRITE (2,*) "square of vector distance (m^2) =", VECTORh
     WRITE (2,*) "number of vectors             =", numvecs

   DO row = 1, nrow
     DO col = 1, ncol
      !  write (6,*) vegcover(row,col)
```

```
  if (row.EQ.378.and.col.EQ.1132) then
   write (4,*) "1",",", row, ",", col,",", ed, ",", fdist,",", vegcover(row,col)
 end if
 if (row.EQ.377.and.col.EQ.1132) then
   write (4,*) "2",",", row, ",", col,",", ed, ",", fdist,",", vegcover(row,col)
 end if
if (row.EQ.381.and.col.EQ.1110) then
   write (4,*) "3", ",",row, ",", col,",", ed, ",", fdist,",", vegcover(row,col)
 end if
if (row.EQ.388.and.col.EQ.1212) then
   write (4,*) "4", ",", row, ",", col,",", ed, ",", fdist,",", vegcover(row,col)
 end if
if (row.EQ.293.and.col.EQ.1094) then
   write (4,*) "5", ",", row, ",", col,",", ed, ",", fdist,",", vegcover(row,col)
 end if
if (row.EQ.348.and.col.EQ.1105) then
   write (4,*) "6", ",", row, ",", col,",", ed, ",", fdist,",", vegcover(row,col)
 end if
if (row.EQ.404.and.col.EQ.1115) then
   write (4,*) "7", ",", row, ",", col,",", ed, ",", fdist,",", vegcover(row,col)
end if
if (row.EQ.385.and.col.EQ.1162) then
   write (4,*) "8", ",", row, ",", col,",", ed, ",", fdist,",", vegcover(row,col)
end if
if (row.EQ.252.and.col.EQ.511) then
   write (4,*) "9", ",", row, ",", col,",", ed, ",", fdist,",", vegcover(row,col)
end if
if (row.EQ.428.and.col.EQ.1126) then
   write (4,*) "10", ",", row, ",", col,",", ed, ",", fdist,",", vegcover(row,col)
end if
```

```
        if (row.EQ.398.and.col.EQ.1285) then
          write (3,*) "11", ",", row, ",", col,",", ed, ",", fdist,",", vegcover(row,col)
        end if
        if (row.EQ.395.and.col.EQ.1299) then
          write (3,*) "12", ",", row, ",", col,",", ed, ",", fdist,",", vegcover(row,col)
        end if
        if (row.EQ.406.and.col.EQ.1299) then
          write (3,*) "13", ",", row, ",", col,",", ed, ",", fdist,",", vegcover(row,col)
        end if
        if (row.EQ.421.and.col.EQ.1323) then
          write (3,*) "14", ",", row, ",", col,",", ed, ",", fdist,",", vegcover(row,col)
        end if
        if (row.EQ.427.and.col.EQ.1336) then
          write (3,*) "15", ",", row, ",", col,",", ed, ",", fdist,",", vegcover(row,col)
        end if
        if (row.EQ.436.and.col.EQ.1321) then
          write (3,*) "16", ",", row, ",", col,",", ed, ",", fdist,",", vegcover(row,col)
        END if
      END DO
    END DO
 END do

END DO
close (1)
STOP
END PROGRAM  airshed
```

Appendix B

Complete tabulation of r^2 values from regression analysis of hobo temperature vs. percent vegetation for all possible airsheds (n = 1512): Temperature = [-0.0155 * (percent land-cover)] + 28.32

Degree Windows (due north = 0°)

r^2	NORTH									EAST								SOUTH
Upwind (m)	1 - 10	11 - 20	21 – 30	31 - 40	41 - 50	51 - 60	61 - 70	71 - 80	81 - 90	91 - 100	101 - 110	111 – 120	121 - 130	131 - 140	141 - 150	151 - 160	161 - 170	171 - 180
30	.40	.40	.41	.43	.43	.47	.57	.57	.57	.40	.40	.43	.57	.57	.59	.57	.57	.57
60	.62	.53	.46	.43	.43	.45	.60	.47	.30	.62	.56	.52	.66	.60	.53	.47	.54	.56
90	.67	.62	.55	.43	.43	.44	.44	.34	.22	.68	.78	.76	.79	.74	.60	.51	.56	.44
120	.78	.64	.54	.43	.43	.44	.42	.23	.25	.79	.84	.80	.73	.70	.53	.51	.51	.45
150	.76	.68	.53	.43	.43	.44	.42	.27	.33	.84	.91	.81	.73	.65	.49	.49	.48	.46
180	.81	.69	.54	.46	.49	.44	.41	.30	.38	.87	.94	.83	.71	.58	.50	.49	.47	.47
210	.83	.74	.52	.41	.48	.46	.45	.40	.48	.91	.92	.78	.69	.59	.51	.55	.48	.47
240	.83	.77	.50	.42	.47	.48	.50	.48	.56	.90	.89	.78	.71	.58	.54	.59	.49	.46
270	.79	.79	.54	.47	.45	.50	.54	.54	.59	.87	.86	.76	.74	.59	.53	.63	.50	.44
300	.78	.79	.59	.50	.46	.49	.54	.56	.60	.84	.83	.73	.76	.62	.53	.62	.52	.41
330	.76	.77	.65	.52	.45	.51	.52	.57	.58	.80	.80	.71	.76	.63	.53	.65	.52	.38
360	.73	.75	.70	.54	.45	.51	.48	.55	.56	.78	.79	.69	.78	.65	.55	.65	.53	.36
390	.71	.74	.68	.54	.44	.47	.43	.52	.54	.76	.78	.70	.79	.67	.58	.66	.54	.37
420	.70	.73	.67	.53	.42	.45	.41	.50	.52	.76	.77	.72	.80	.69	.60	.67	.54	.38
450	.71	.71	.68	.52	.40	.43	.38	.47	.49	.75	.79	.75	.83	.71	.62	.68	.54	.38
480	.73	.71	.69	.50	.38	.41	.38	.45	.46	.76	.81	.76	.83	.73	.63	.66	.55	.38
510	.74	.72	.70	.49	.36	.39	.38	.44	.44	.79	.82	.76	.82	.75	.64	.64	.55	.38
540	.76	.71	.70	.48	.35	.40	.35	.44	.43	.81	.83	.76	.81	.75	.67	.65	.54	.38
570	.77	.71	.68	.48	.35	.40	.33	.43	.43	.80	.83	.76	.80	.75	.68	.65	.55	.38
600	.78	.70	.67	.47	.34	.38	.32	.43	.44	.79	.82	.76	.78	.75	.69	.65	.54	.38
630	.77	.69	.65	.46	.34	.36	.30	.42	.45	.77	.82	.76	.76	.73	.68	.64	.54	.38

660	.77	.68	.64	.46	.33	.34	.30	.41	.45	.78	.81	.76	.73	.71	.68	.65	.53	.38
690	.78	.68	.63	.46	.32	.33	.30	.40	.44	.79	.80	.76	.71	.69	.68	.66	.52	.37
720	.80	.68	.62	.46	.31	.31	.29	.39	.45	.80	.79	.75	.68	.67	.67	.66	.53	.38
750	.81	.69	.63	.47	.31	.31	.28	.39	.47	.82	.79	.75	.64	.66	.66	.67	.54	.39
780	.82	.70	.64	.47	.30	.29	.25	.37	.47	.83	.80	.75	.62	.65	.64	.67	.54	.40
810	.83	.71	.64	.48	.30	.28	.23	.36	.47	.84	.80	.74	.61	.65	.63	.66	.54	.41
840	.83	.72	.65	.49	.30	.27	.20	.35	.47	.85	.80	.73	.60	.64	.62	.65	.55	.42
870	.83	.72	.65	.49	.31	.26	.19	.34	.48	.86	.79	.72	.60	.64	.61	.64	.56	.44
900	.83	.72	.65	.49	.31	.26	.19	.35	.49	.87	.79	.71	.59	.64	.60	.64	.57	.45
930	.82	.72	.64	.49	.31	.27	.20	.37	.50	.87	.77	.71	.57	.63	.59	.63	.57	.46
960	.81	.71	.63	.48	.32	.27	.22	.38	.52	.88	.76	.71	.56	.63	.59	.63	.57	.47
990	.80	.71	.62	.48	.32	.28	.23	.40	.53	.87	.74	.71	.53	.61	.59	.63	.57	.48
1020	.78	.71	.62	.48	.32	.29	.24	.41	.54	.87	.73	.69	.51	.60	.59	.63	.58	.49
1050	.76	.70	.62	.47	.33	.30	.25	.42	.56	.86	.71	.68	.49	.57	.59	.63	.59	.49
1080	.75	.70	.62	.47	.33	.30	.26	.43	.56	.86	.70	.66	.48	.56	.58	.62	.60	.51
1110	.73	.69	.62	.46	.34	.31	.28	.43	.57	.86	.70	.65	.47	.54	.58	.61	.60	.52
1140	.71	.68	.61	.46	.34	.32	.29	.43	.57	.85	.69	.63	.45	.53	.58	.60	.61	.52
1170	.69	.68	.60	.46	.35	.32	.31	.44	.57	.85	.68	.62	.42	.52	.58	.59	.61	.52
1200	.67	.68	.59	.46	.35	.33	.32	.44	.56	.83	.68	.60	.41	.50	.57	.59	.61	.53
1230	.66	.68	.58	.45	.35	.33	.33	.45	.56	.82	.67	.59	.39	.49	.57	.59	.60	.54
1260	.64	.68	.58	.44	.35	.33	.34	.45	.56	.80	.66	.57	.37	.48	.57	.59	.61	.54
1290	.63	.68	.58	.43	.35	.33	.35	.45	.56	.78	.64	.55	.35	.46	.56	.59	.60	.55
1320	.61	.69	.57	.42	.34	.33	.36	.46	.56	.76	.62	.54	.33	.45	.56	.60	.61	.55
1350	.60	.69	.57	.41	.33	.33	.36	.46	.56	.74	.61	.53	.32	.44	.55	.60	.61	.55
1380	.58	.70	.58	.41	.33	.34	.36	.45	.56	.73	.60	.53	.30	.43	.54	.61	.61	.55
1410	.56	.70	.58	.40	.34	.34	.37	.46	.56	.71	.60	.53	.30	.43	.53	.62	.62	.55
1440	.55	.70	.58	.40	.35	.35	.39	.46	.56	.69	.59	.53	.30	.43	.53	.62	.62	.56
1470	.54	.71	.58	.39	.36	.36	.40	.47	.56	.67	.59	.53	.30	.44	.53	.63	.63	.56
1500	.53	.71	.58	.39	.36	.37	.41	.47	.56	.65	.58	.53	.30	.45	.53	.63	.64	.57
1530	.52	.71	.58	.39	.37	.38	.42	.48	.57	.62	.59	.54	.30	.46	.53	.64	.64	.57
1560	.51	.71	.59	.39	.38	.39	.42	.48	.57	.60	.59	.54	.29	.46	.53	.65	.65	.58
1590	.51	.71	.59	.39	.38	.39	.43	.48	.57	.58	.60	.55	.29	.46	.53	.65	.65	.58

1620	.50	.71	.60	.39	.39	.40	.44	.49	.58	.58	.60	.55	.29	.46	.53	.66	.65	.58
1650	.51	.71	.60	.39	.39	.41	.45	.49	.58	.57	.60	.55	.28	.45	.52	.66	.66	.59
1680	.51	.71	.61	.40	.39	.41	.46	.49	.57	.57	.60	.55	.28	.44	.52	.67	.66	.59
1710	.51	.70	.61	.41	.40	.42	.46	.50	.57	.57	.60	.55	.28	.43	.52	.67	.66	.59
1740	.51	.70	.62	.41	.40	.42	.47	.50	.57	.56	.60	.56	.27	.42	.52	.68	.66	.60
1770	.52	.70	.62	.42	.40	.43	.47	.50	.57	.56	.61	.56	.27	.41	.53	.68	.67	.60
1800	.52	.70	.62	.42	.40	.43	.48	.51	.57	.55	.60	.57	.27	.40	.53	.69	.67	.60
1830	.52	.70	.62	.42	.40	.43	.48	.52	.57	.54	.60	.57	.27	.40	.54	.69	.67	.60
1860	.52	.70	.62	.42	.41	.43	.49	.52	.57	.54	.60	.58	.27	.40	.54	.70	.67	.60
1890	.52	.69	.62	.43	.41	.43	.50	.52	.57	.53	.59	.58	.28	.40	.55	.70	.67	.60
1920	.52	.69	.62	.43	.40	.43	.51	.52	.57	.52	.59	.59	.28	.40	.55	.70	.68	.60
1950	.52	.69	.62	.43	.40	.43	.51	.53	.57	.52	.59	.59	.28	.41	.55	.69	.68	.61
1980	.52	.68	.63	.42	.40	.43	.52	.53	.56	.51	.60	.60	.29	.41	.55	.69	.68	.61
2010	.52	.68	.63	.42	.39	.43	.52	.53	.56	.50	.60	.60	.30	.41	.54	.69	.68	.61
2040	.52	.68	.63	.42	.38	.43	.53	.53	.55	.49	.61	.60	.30	.41	.54	.69	.68	.61
2070	.52	.68	.63	.42	.38	.43	.53	.52	.55	.49	.61	.60	.31	.42	.54	.69	.68	.61
2100	.52	.67	.63	.41	.37	.43	.54	.52	.55	.48	.61	.60	.32	.42	.54	.69	.68	.62
2130	.52	.67	.63	.41	.37	.42	.54	.52	.55	.48	.61	.60	.31	.43	.54	.69	.68	.62
2160	.51	.67	.63	.40	.36	.42	.55	.52	.54	.48	.61	.60	.31	.43	.55	.69	.68	.62
2190	.51	.67	.63	.40	.36	.42	.55	.52	.54	.48	.61	.60	.32	.44	.55	.68	.67	.62
2220	.51	.67	.63	.40	.35	.42	.56	.52	.54	.47	.61	.60	.33	.44	.55	.68	.68	.62
2250	.51	.67	.63	.40	.35	.42	.56	.52	.53	.47	.61	.60	.34	.44	.55	.68	.67	.62
2280	.51	.67	.63	.40	.34	.43	.57	.52	.53	.47	.60	.60	.35	.45	.55	.68	.67	.62
2310	.52	.67	.63	.41	.34	.43	.57	.52	.53	.47	.60	.60	.36	.45	.55	.67	.67	.63
2340	.52	.67	.63	.41	.34	.43	.57	.52	.52	.46	.60	.60	.36	.45	.55	.67	.67	.63
2370	.52	.67	.64	.41	.34	.44	.58	.52	.52	.46	.59	.61	.37	.45	.55	.67	.66	.63
2400	.52	.67	.64	.42	.34	.44	.58	.52	.52	.45	.59	.61	.37	.45	.54	.66	.66	.63
2430	.53	.67	.64	.42	.34	.45	.58	.53	.52	.45	.59	.62	.38	.45	.54	.66	.66	.63
2460	.53	.68	.64	.43	.34	.45	.58	.53	.52	.45	.58	.63	.39	.45	.54	.66	.66	.63
2490	.53	.67	.65	.43	.35	.45	.58	.53	.53	.44	.57	.63	.39	.45	.53	.65	.66	.63
2520	.53	.67	.65	.43	.35	.46	.59	.54	.53	.44	.57	.64	.39	.45	.53	.65	.66	.63

VITA

David J. R. Murphy

Date of Birth: 7-18-1981
Place of Birth: Morristown, New Jersey

Education	Name and Location:	Dates:	Degree:
High School:	Seton Hall Preparatory West Orange, New Jersey	9/95 – 6/99	
College:	College of the Holy Cross Worcester, Massachusetts	9/99 – 5/03	B.A. - Biology
Graduate School:	SUNY – College of Environmental Science and Forestry Syracuse, New York	9/04 – 5/07	M.S. - Environmental Science

Employment	Employer:	Dates:	Job Title:
	Research Foundation of New York	02/06 – 03/07	Graduate Research Assistant
	SUNY – College of Environmental Science and Forestry	08/04 – 12/04 08/05 – 12/05	Teaching Assistant for Urban Ecology
	Birch Wathen Lenox School	08/03 – 07/04	Full-Time Middle and Upper School Faculty Member